

Research Papers
Issue RP0265
November 2015

*Regional Models and
geo-Hydrological Impacts
Division*

Climate-Hydrological Modelling of Calore Irpino River Basin

By Renata Vezzoli

Regional Models and
geo-Hydrogeological Impacts
Division, CMCC - Capua
renata.vezzoli@cmcc.it

Paola Mercogliano

Meteo System &
Instrumentation Laboratory,
CIRA - Capua Regional Models
and geo-Hydrogeological
Impacts Division, CMCC -
Capua
p.mercogliano@cira.it

and Valentina Coppola

Regional Models and
geo-Hydrogeological Impacts
Division, CMCC - Capua
valentina.coppola@cmcc.it

SUMMARY This paper provides the main results about the climate-hydrological modelling of Calore Irpino River basin in Southern Italy under current and future climate conditions. This test case represents a further application of the modelling chain presented in [40] and of climate projections introduced in [18, 3, 42] within the Work Package A.2.17 "Analysis of geological risk related to climate change" of GEMINA project.

Keywords: Modelling, Climate, Hydrology, Basin, Calore Irpino

*This report is developed
within the framework of
Work Package 2.17
Action A of the GEMINA
Project, funded by the
Italian Ministry of
Education, University and
Research and the Italian
Ministry of Environment,
Land and Sea. The
authors will thank the
Functional Center of
Campania Region for
kindly providing the
observed dataset used in
this work. The authors
will thank Prof. Giugni for
the useful advices and
support.*



1. INTRODUCTION AND MOTIVATION

The majority of the climate models agrees in expecting at 2100, under the effect of climate change, an increase in extreme precipitation events frequency and almost unchanged intensity, and, on average, a decrease in the total precipitation over the Mediterranean area [6]. The expected partitioning of precipitation enhances the possibility of an alternation between long dry and short extremely wet periods [2], causing, generally, an increase in the geo-hydrological hazards frequency or severity. In last years, REMHI Division among others [8, 4, 13, 22], has investigated the potential effects of climate change on geo-hydrological hazards in Italian Peninsula [36, 35, 37, 7, 21, 23, 24, 9] that is already prone to them and the main results achieved have been presented in [19].

This work presents the step by step implementation of a climate-hydrological modeling chain over the Calore Irpino River basin in Southern Italy, that, recently (October 2015), hits the headlines since it flooded the city of Benevento causing fatalities and huge economic damages.

The report is structured as follows: Section 2 provides a brief description of the test case area; Section 3 presents the hydrological model used; Section 4 provides the results of the sensitivity, calibration and validation analysis; Section 5 describes the available climate simulations and bias correction approaches; in Section 6 climate data are used to drive the hydrological model under present an future climate conditions while Section 7 is dedicated to the analysis of extreme discharges, as last, in Section 8 results are commented and main conclusions are drawn.

2. CALORE IRPINO TEST CASE

The Calore Irpino River basin covers an area of about 3058 km² in Campania, Fig. 1. The river

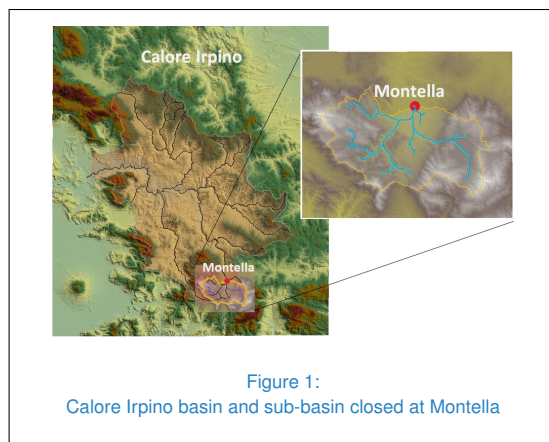
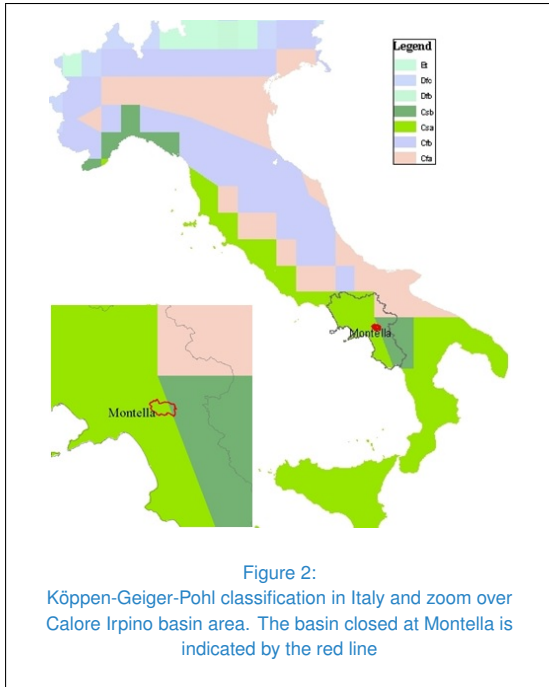


Figure 1:
Calore Irpino basin and sub-basin closed at Montella

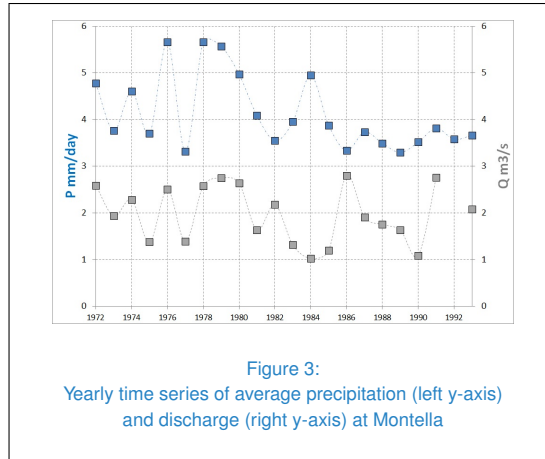
length is about 108 km and the average discharge is 31.8 m³/s at its outlet in the Volturno River. The Calore Irpino River basin is characterised by a micro-climate that, together with the water availability guarantee by the river itself, foster the cultivation of vegetables, vineyard and olive trees. The occurrence of climate changes may alter the equilibrium of this ecosystem with impacts on the local economy.

Calore Irpino basin is characterized by Mediterranean climate with hot and dry summers and cold winters. More in details, the climate is wet from autumn to spring and dry in summer. On average, the monthly precipitation is maximum in November and minimum in July. According to Köppen-Geiger-Pohl classification the basin falls into zones Csa and Csb (Fig. 2) with dry summers, i.e. the precipitation of at least one month in summer is less than 30 mm and of 1/3 of the precipitation in the wettest winter month; and average temperature is above 10°C in summers and in the warmest month is above 22°C; during winters the average temperature ranges between -3 and 18°C; and, as last, at least four (Csa) or two (Csb) months show a temperature above 10°C.

The test case is a limited to the portion of the basin defined by Montella river cross section, reducing the test case area to about



110 km². The choice of this limited portion of domain is related to the availability of meteorological and hydrological data on Montella site and to absence of documented water uptakes from this river branch. Observed daily precipitation (1972-2001) and temperature (1972-1994) data are available from Part I of Hydrological YearBooks or, upon request, from Campania Regional Civil Protection and have been tested for homogeneity and trend in Clime [5]. Observed daily discharge (1972-1993) data are available from Part II of Hydrological YearBooks; for the following periods data were not available: August-September 1975, October 1979-April 1980, February-May 1984 and 1985; January and August-November 1986, July-August and October 1988, March-May 1989, January 1981 and the whole 1992. Calore Irpino discharges in the upper part of the basin, i.e. in proximity of Montella station, follow the precipitation pattern with low/minimum discharges in summer (also due to the high evapotranspiration) and autumn and the highest dis-



charges occurring between winter and spring.

To calibrate the hydrological model the period 1972-1982 will be used, while the remaining years will be used to validate the calibration. In addition, across the years 1980-1986, a change in hydrological response to precipitation (precipitation-discharge relationship) is observed but any metadata was available to help us in understanding this phenomenon, see Fig. 3; this fact will make complex the validation of the hydrological model.

3. HYDROLOGICAL MODEL

3.1 DESCRIPTION

In this work, a fully-distributed physically-based hydrological model TOPKAPI (TOPographic Kinematic APproximation and Integration, [16]) is used to simulate the Calore Irpino hydrological response to present and future climate conditions. TOPKAPI simulates the main component of the hydrological cycle such as surface flow, soil drainage, evapotranspiration, snow melting, etc. . . . According to the description in [16]: *TOPKAPI couples the kinematic approach with the topography of the basin and transfers the rainfall-runoff processes into three structurally-similar zero-dimensional non-linear reservoir equations: the first represents the drainage in the soil, the*



second the overland flow on saturated or impervious soils and the third the channel flow. The parameters of the model are shown to be scale independent and obtainable from digital elevation maps, soil maps and vegetation or land use maps in terms of slopes, soil permeability, topology and surface roughness. The integration of the fundamental equations is performed on the individual cell of the DEM. [. . .] In each cell, five water components are considered: evapotranspiration, snowmelt, soil water, surface water and channel water. For the deep aquifer flow, the response time caused by the vertical transport of water through the thick soil above this aquifer is so large that horizontal flow in the aquifer can be assumed to be almost constant with no significant response on one specific storm event in a catchment [30]. Nevertheless, the model accounts for water percolation towards the deeper subsoil layers even though it does not contribute to the discharge. As precipitation falls on the catchment, the snow accumulation and melting component identifies the amount of water that actually reaches the soil surface. For reasons of limited data availability, the snow accumulation and melting (snowmelt) component is driven by a radiation estimate based upon air temperature measurements. Once water is on the soil surface, it infiltrates unless the soil is already saturated. The soil water component is affected by subsurface flow (or interflow) in a horizontal direction defined as drainage; drainage occurs in a surface soil layer, with limited thickness and with high hydraulic conductivity due to its macro porosity. The drainage mechanism plays a fundamental role in the model both as a direct contribution to the flow in the drainage network and most of all as a factor regulating the soil water balance, particularly in activating the production of overland flow. The soil water component is the most characterizing aspect of the model because it regulates the functioning of the contributing saturated areas. The surface water component is activated on the basis of this mechanism. Lastly, both components contribute to feeding the drainage network. The

evapotranspiration is taken into account as water loss, subtracted from the soil's water balance. The most complex and physically realistic model for estimating actual evapotranspiration is the Penman-Monteith equation. However, a simplified approach is generally necessary because in many countries the required historical data for Penman-Monteith estimations are not extensively available; and, in addition, apart from a few meteorological stations, almost nowhere are real-time data available for flood forecasting applications. Evapotranspiration plays a major role not in terms of its instantaneous impact, but in terms of its cumulative temporal effect on the soil moisture volume depletion; this reduces the need for an extremely accurate expression, provided that its integral effect is well preserved. In the present TOPKAPI model, evapotranspiration can be introduced directly as an input to the model or computed internally by a radiation method [10] starting from air temperature and from other topographic, geographic and climatic information, as described in the ARNO model [31].

3.2 MODEL IMPLEMENTATION

The implementation of an hydrological model in TOPKAPI requires the following information: digital elevation model (DEM), land use/cover and soil type to build the soil model and the hydrological network, that can be validated by comparison with the observed network; to perform the hydrological simulations geo-referred time series of precipitation and air temperature are requested, if needed localized water releases/uptakes can be inserted in the model. TOPKAPI outputs include among others: discharge, evaporation, runoff, soil saturation time series that can be used to validate the model with respect to observations.

For Calore Irpino test case a DEM of 5m horizontal resolution will be used to discretize the domain into more than 11000 square cells of 100 m side, corresponding to 112



rows and 173 columns. Land cover data are available from CORINE Land Cover 2006 <http://www.sinanet.isprambiente.it/it/sia-ispra/download-mais/corine-land-cover/corine-land-cover-2006/view> dataset. In the test case area 10 different types of land cover are identified, see Fig. 4. Each land cover type is parametrized in terms of soil surface roughness (Manning's Coefficients for soil surface roughness n_c in $\text{s/m}^{1/3}$) and actual evapo-transpiration with respect to the crop reference potential evapo-transpiration value (crop factor K_c adimensional and varying month by month). Manning's coefficient is relevant to estimate the superficial runoff and its timing.

The soil properties are derived from the FAO Digital Soil Map of the World, thus this data is quite coarse and only the soil type "Bd68-2bc" to which corresponds to eruptive and metamorphic rock, sandstone, eruptive rock is retrieved in sub-basin Calore Irpino. The following parameters are used to describe the hydraulic properties of each soil type:

- Horizontal permeability at saturation (K_s in m/s),
- Vertical permeability at saturation (K_{sv} in m/s),
- Vertical non-linear reservoir exponent (α_p adimensional),
- Horizontal non-linear reservoir exponent (α_s adimensional),
- Depth of the superficial soil layer (L in m),
- Saturated water content (Θ_s adimensional),
- residual water content (Θ_r adimensional).

Once the model is configured it has to be calibrated and validated: the calibration phase aims to identify the parameters values combination that allow to better reproduce the observed discharges; the validation phase aims to verify the model performances over and independent time period using the parameters values defined in calibration. In the next Section, the results of calibration and validation of TOPKAPI for Calore Irpino test case are presented.

4. ESTIMATION OF PARAMETERS VALUE

Physically based hydrological models should not need to be calibrated since parameters values should be related directly with catchment characteristics [26]. Unfortunately, the quality/quantity/variety of catchments data allows to set a variability range for parameters but it is not sufficient to fix their value. For this reason a sensitivity analysis to parameters values is needed to evaluate their weight on the results of a simulation. Once assessed the weight of each parameter, it is possible to calibrate the model and then validate the selected parameters values. In the following paragraphs the results of sensitivity analysis, calibration and validation activities are described.

4.1 SENSITIVITY ANALYSIS

TOPKAPI model uses non-linear kinematic wave equations, therefore is difficult to estimate directly the effects of changes in the parameters' values and identify whose are the most relevant. The sensitivity analysis has been performed over the period 1972-1982 forcing TOPKAPI with observed precipitation and temperature time series varying one parameter at the time. In particular, the sensitivity analysis focused on the following parameters:

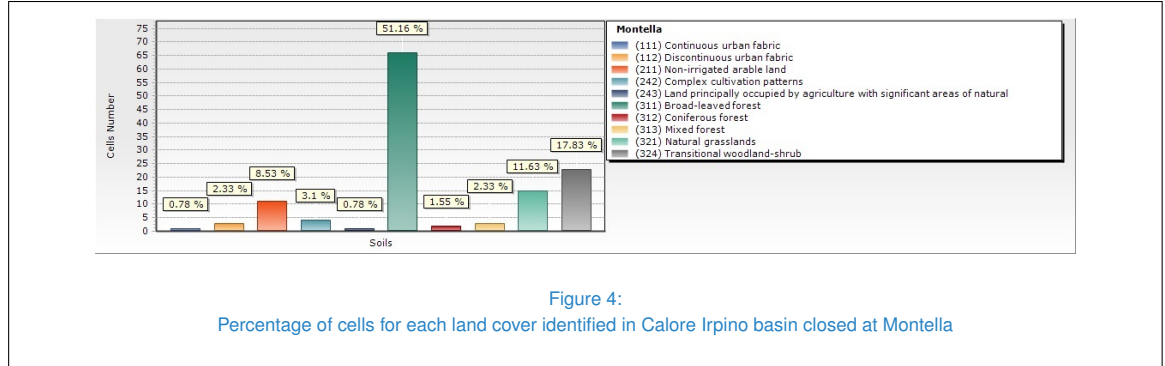


Figure 4: Percentage of cells for each land cover identified in Calore Irpino basin closed at Montella

- Horizontal permeability at saturation (K_s),
- Vertical permeability at saturation (K_{sv}),
- Vertical non-linear reservoir exponent (α_p)
- Soil depth (L)
- Manning's friction coefficient for the channel roughness (n_c)
- Manning's coefficients for soil surface roughness (n_o).

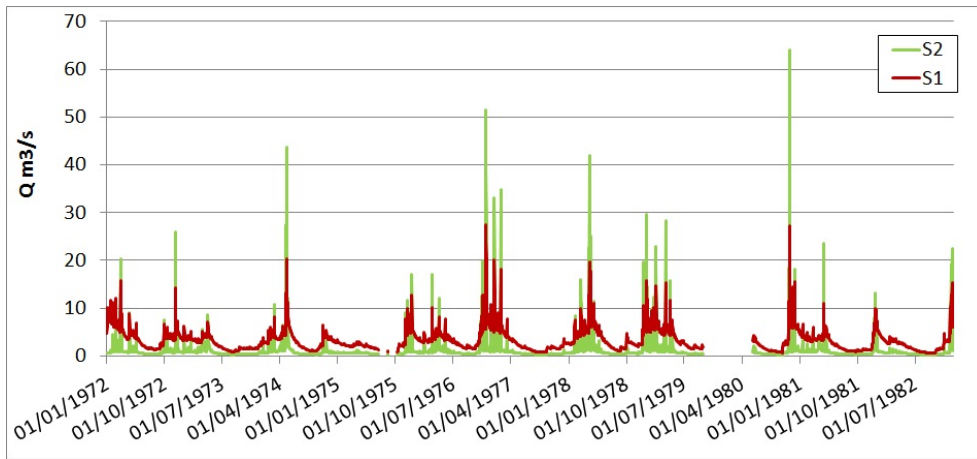
Horizontal permeability at saturation depends on soil characteristics and regulates the amount of water moving horizontally in the soil superficial layer, S1 run refer to $K_s = 8 \cdot 10^{-5}$ m/s case and S2 run to $K_s = 10^{-5}$ m/s case; results show that a reduction of K_s corresponds to a decrease in soil drainage while surface runoff increases and, thereby, the peak discharge. Figure 5(a) reports the comparison between S1 and S2 where S2 is characterized by lower minimum discharges and higher maxima with respect to S1. The comparison among the monthly average observed, S1 and S2 discharges indicates that K_s values should fall into the $10^{-5} - 8 \cdot 10^{-5}$ m/s range, Fig. 5(b).

Vertical permeability at saturation (K_{sv}) is related to percolation process and regulates the amount of water moving vertically in the soil superficial layer. For this parameter the following

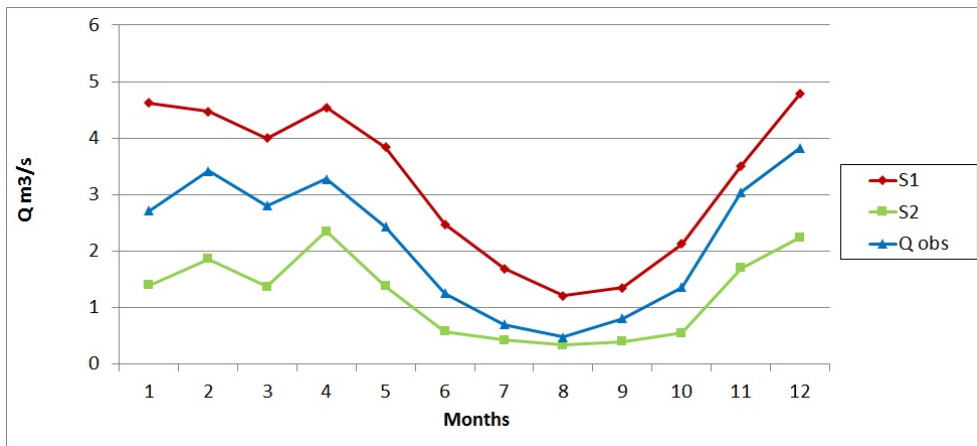
values have been tested: 10^{-8} (run S3) and $2 \cdot 10^{-7}$ m/s (run S4). The resulting discharges are reported in Fig. 6(a) while Fig. 6(b) provides the comparison among simulated and observed monthly average discharges. An increase of K_{sv} value causes an increase in percolation and a decrease in discharge.

Vertical non-linear reservoir exponent (α_p) rules the percolation too and it is a function of the soil type. Calore Irpino basin soil type is classified as sand/clay, for this soil type α_p usually ranges between 11 and 25. However, experimentally, we find that reliable results are achieved for α_p varying between 3 (S5) and 20 (S6). Increases in this parameter value generate decrease in percolation and increase in discharge. It is worth to note that TOPKAPI appears to be more sensitive to changes in vertical permeability at saturation parameter than to changes in vertical non-linear reservoir exponent. Figure 7 reports the same comparison of Fig. 5.

The depth of the superficial soil layer L regulates the maximum amount of water stored in the soil superficial layer and it influences the amount of water moving horizontally (drainage) and vertically (percolation) into the soil. Simulations S7 and S8 provide the results for $L = 1$ and $L = 3$ m respectively, Fig. 8(a)-(b), the comparison is analogue to Fig. 5(a)-(b). Changes in L affects the soil water storage capacity: the less L is the more surface runoff

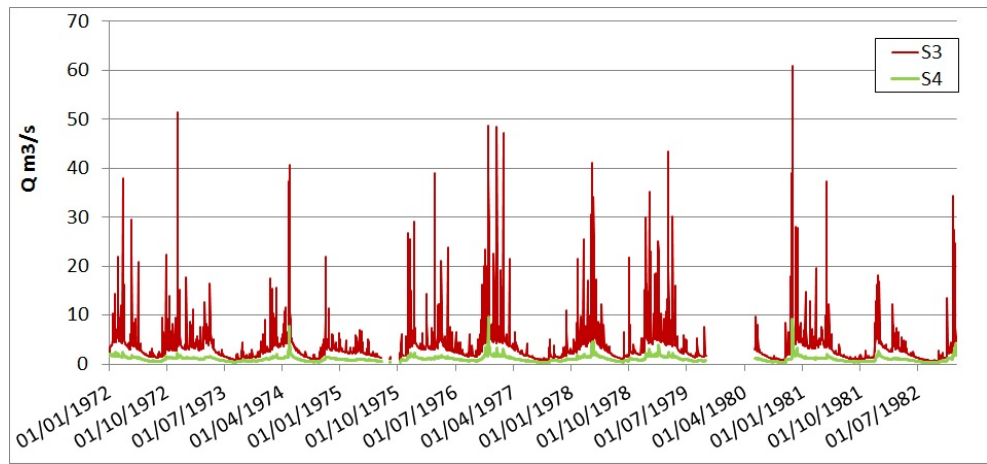


(a)

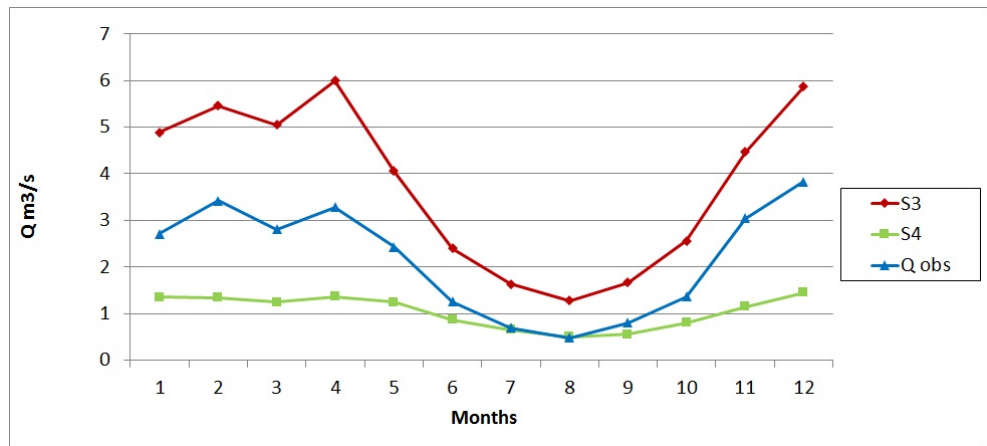


(b)

Figure 5:
Comparison among observed and simulated daily discharge time series (a) and monthly averages (b) for two different values of K_s , see text

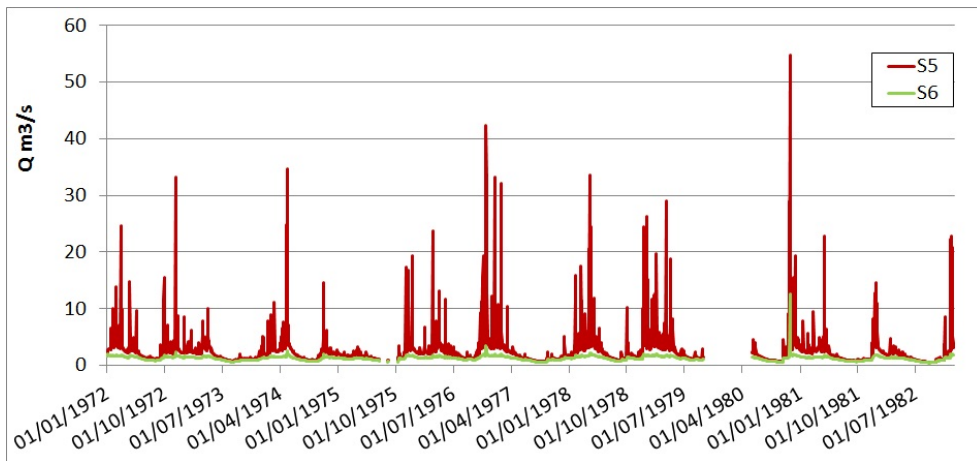


(a)

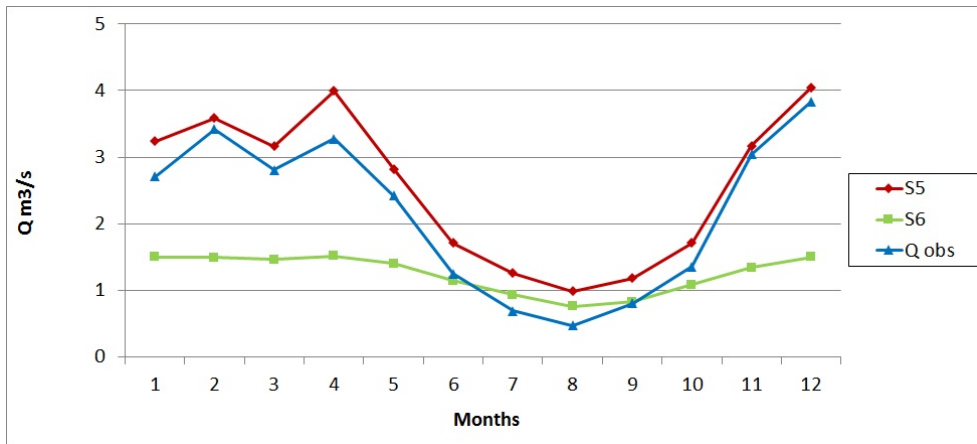


(b)

Figure 6:
As Fig. 5 but for two different values of K_{sv}



(a)



(b)

Figure 7:
As Fig. 5 but for two different values of α_p



and its propagation and peak discharge are.

Manning's friction coefficient for the channel roughness (n_c) influences the flow in open channels, a reduction of the parameter value reduces the discharge. Figure 9 reports the results the comparison in terms of daily and monthly average discharges for S9, $n_c = 0.01$ s/m^{1/3}, and S10, $n_c = 0.12$ s/m^{1/3}, runs. The analysis of Fig. 9(b) shows that TOPKAPI is not very sensitive to this parameter.

Manning's Coefficients for soil surface roughness n_o in s/m^{1/3} regulates the celerity and the shape of overland discharge waves and it is a function of the land cover. For the test case we performed the sensitivity analysis only for the parameter associated to the dominant land cover, i.e broad leaved forest (311). In particular the values 0.28 s/m^{1/3} and 0.1 s/m^{1/3} are tested in runs S11 and S12 respectively, the comparison is shown in Fig. 10; the resulting discharges are comparable.

The sensitivity analysis returns the indication to concentrate the calibration efforts on the following parameters: Horizontal Permeability at Saturation, vertical Permeability at Saturation and Vertical Non-Linear Reservoir Exponent.

4.2 CALIBRATION AND VALIDATION

The calibration of TOPKAPI model for Calore Irpino basin closed at Montella has been performed over the 11-years long period 01/01/1972 and 31/12/1982 using daily precipitation and temperature time series as inputs and daily discharge time series as control variable. The length of the calibration period is in agreement with literature suggestions/requirements [39] and it include both dry and wet prolonged periods.

According to the sensitivity analysis the calibration mostly focused on the following parameters:

- Horizontal permeability at saturation (K_s)
- Vertical permeability at saturation (K_{sv})
- Vertical non-Linear reservoir exponent (α_p)

Several simulations have been performed to search the best parameters combinations. Table 1 reports some of the parameters combination tested which results will be illustrated in this paragraph. In simulations belonging to groups A, C and E the values of the horizontal permeability at saturation and vertical non-linear reservoirs exponent have been fixed while the vertical permeability at saturation is varying, in group D horizontal and vertical permeability at saturation have been kept constant and vertical non-linear reservoirs exponent varies. The first criterion applied to select the "best" parameters configuration among those tested is the equality between observed ($RUNOFF_{obs}$) and simulated ($RUNOFF_{tpk}$).

The performances of the selected simulations have been compared through a set of statistical indices as indicated in [16]:

- Mean absolute error (MAE) it varies between 0.0 and $+\infty$

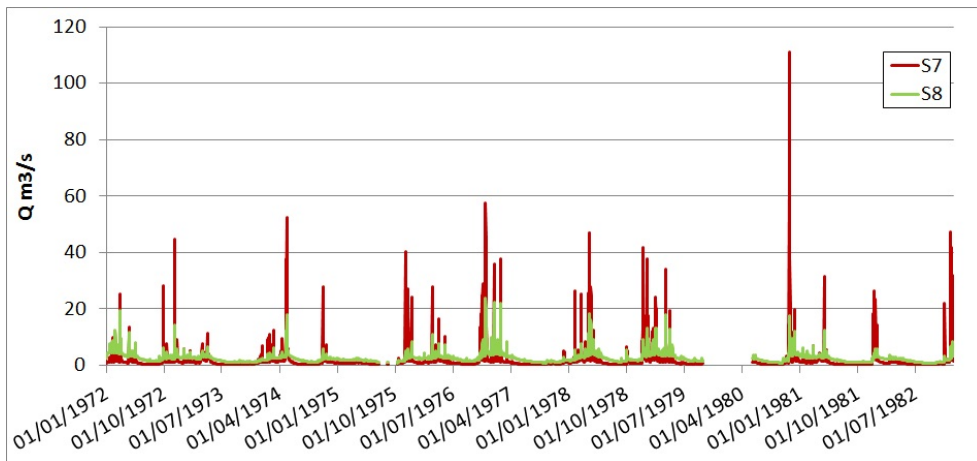
$$MAE = \frac{|\sum_{i=1}^N (Q_{obs}(i) - Q_{sim}(i))|}{N}, \quad (1)$$

- Mean square error (MSE) it varies between 0.0 and $+\infty$,

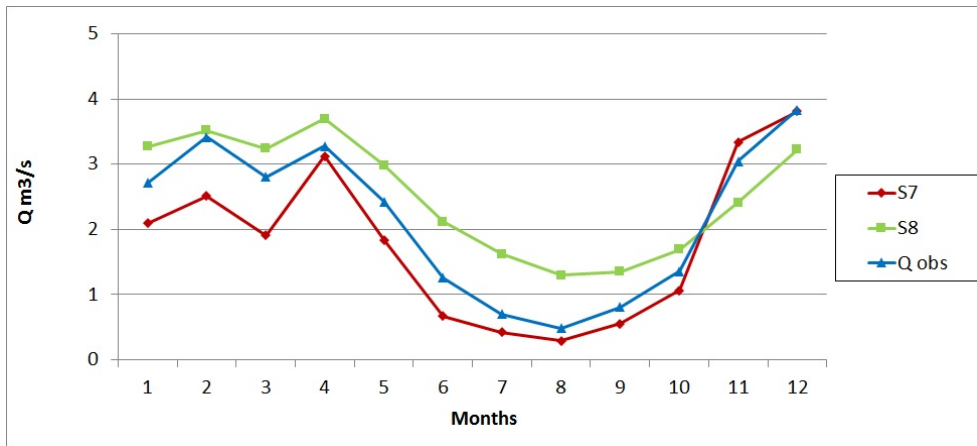
$$MSE = \frac{\sum_{i=1}^N (Q_{obs}(i) - Q_{sim}(i))^2}{N}, \quad (2)$$

- Root mean square error (RMSE) it varies between 0 and $+\infty$,

$$RMSE = \sqrt{\frac{\sum_{i=1}^N (Q_{obs}(i) - Q_{sim}(i))^2}{N}} \quad (3)$$

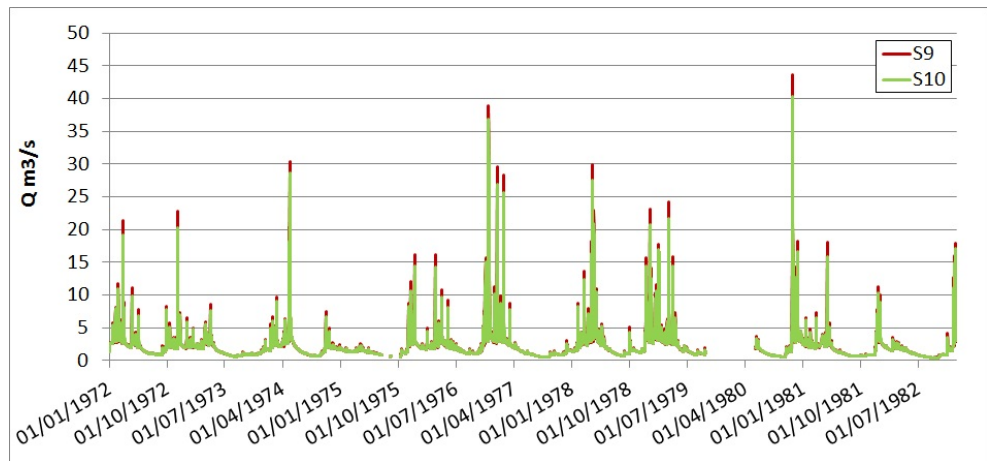


(a)

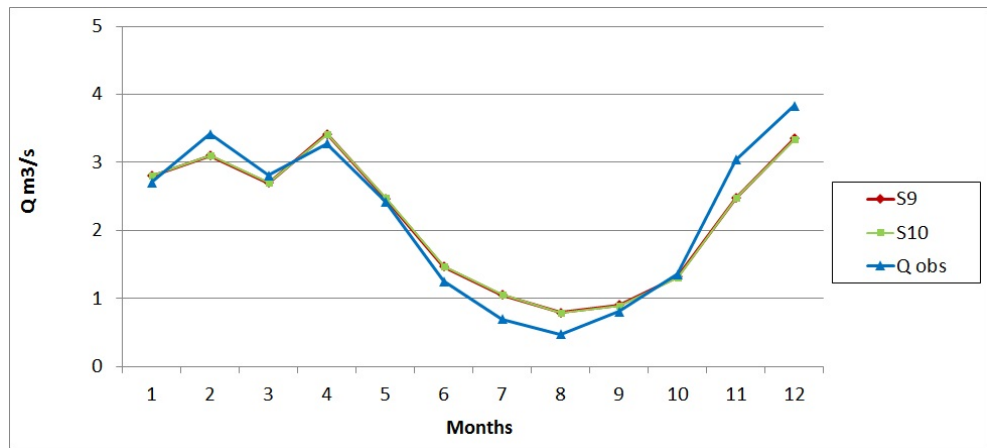


(b)

Figure 8:
As Fig. 5 but for two different values of L

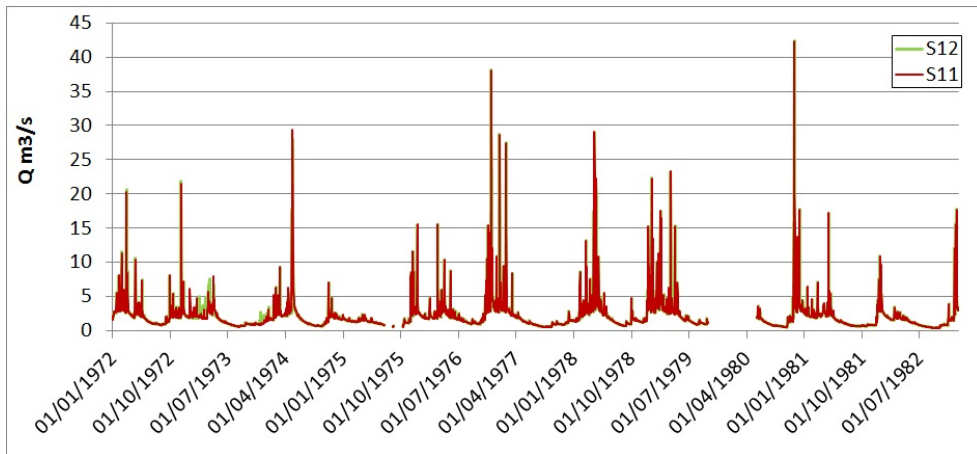


(a)

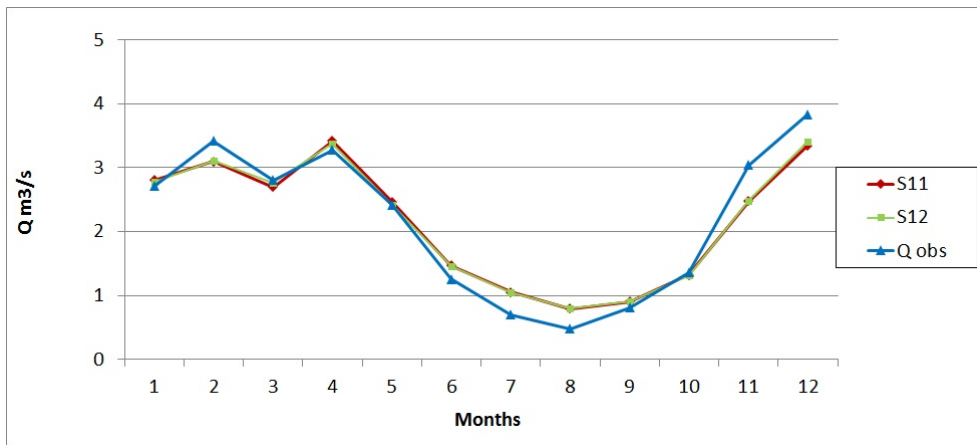


(b)

Figure 9:
As Fig. 5 but for two different values of n_c



(a)



(b)

Figure 10:
As Fig. 5 but for two different values of n_c



Test	Horizontal Permeability at Saturation [$10^{-5}m/s$]	Vertical Permeability at Saturation [$10^{-8}m/s$]	Vertical Non-Linear Reservoir Exponent [-]	RUNOFF _{obs} coeff. [-]	RUNOFF _{tpk} coeff. [-]	Discharge [%]	Percolation [%]
A1	1.09	3	20	38.14	47.21	47.22	21.90
A2	1.09	4	20	37.68	42.10	42.11	27.08
A3	1.09	5	20	37.28	37.81	37.81	31.42
C2	4	6	3	37.14	37.70	37.25	37.75
C3	4	6.5	3	36.99	35.42	35.42	39.72
C4	4	7	3	36.85	34.16	33.72	41.54
D1	4	6.5	5	37.11	36.91	36.69	36.74
D2	4	6.5	5	37.19	37.90	37.69	35.61
D4	4	6.5	6	37.27	38.76	38.55	34.63
D5	4	6.5	8	37.48	41.29	41.10	31.81
D6	4	6.5	12	37.72	44.13	43.95	28.72
E1	2	6.5	12	37.19	37.38	37.38	34.02
E2	2	6	12	37.33	38.96	38.96	32.39
E3	2	4	12	28.01	46.67	46.67	24.53
E4	2	3	12	38.44	51.49	41.50	19.63

Table 1
Parameters values used in calibration

- Coefficient of determination (R2) ranges from 0.0 (poor model) to 1.0 (perfect model),

$$R2 = \frac{\sum_{i=1}^N (Q_{obs}(i) - \overline{Q_{obs}})(Q_{sim}(i) - \overline{Q_{sim}})}{\sqrt{\sum_{i=1}^N (Q_{obs}(i) - \overline{Q_{obs}})^2} \sqrt{\sum_{i=1}^N (Q_{sim}(i) - \overline{Q_{sim}})^2}}, \quad (4)$$

- Nash-Sutcliffe (NS) ranges from $-\infty$ (poor model) to 1.0 (perfect model)

$$NS = 1 - \frac{\sum_{i=1}^N (Q_{obs}(i) - Q_{sim}(i))^2}{\sum_{i=1}^N (Q_{obs}(i) - \overline{Q_{obs}})^2}. \quad (5)$$

where $Q_{obs}(i)$ and $Q_{sim}(i)$ are the i -th observed and simulated value, respectively, $\overline{Q_{obs}}$ and $\overline{Q_{sim}}$ are the average observed and simulated values, respectively and N is the sample size.

In particular, MSE and RMSE are equally affected by errors in high and low flows while R2, that describes the proportion of the total variance in the observed data that can be explained by the model, and NS, indicates if the model is a better predictor than the average value, both R2 and NS are sensitive to errors in high flows. For NS index a value equal zero indicates that

the model is a good predictor as well as the average observed value, $NS < 0$ indicate that the observed average values is a better predictor than the model, $0 < NS \leq 0.2$ the model performances are insufficient; $0.2 < NS \leq 0.4$ the model is sufficient, $NS > 0.4$ means good or very good ($NS > 0.6$) performances.

Table 2 reports the values of indices RMSE, RMSE-MAE, R2 and NS for the four simulations that respects the criterion of equality between $RUNOFF_{obs}$ and $RUNOFF_{tpk}$ in Tab. 1. The use of RMSE-MAE index allows to out into evidence the presence of outliers into the data.

The coefficient of determination R2 shows a limited variability within the four simulations considered so it does not provide key information to the choice of the “best” parameter combination. The values of NS index indicate



Run	RMSE	RMSE-MAE	R2	NS
A3	3.5	2.2	0.87	-0.74
C2	3.9	1.1	0.85	0.53
D1	1.7	0.8	0.88	0.61
E2	2.4	2.4	0.86	0.29

Table 2

Statistical indices for four calibration simulations

that only simulations C2 and D1 are good predictors, and between them simulation D1 outperform simulation C2 according to RMSE and RMSE-MAE values. Thus D1 results to be the "best" calibration among those tested (Fig. 11).

The validation of D1 parameters set is carried on over the period 1983-1993. Figure 12 reports the comparison between observed and simulated monthly average discharges in the validation period. It is easy to note that, with respect to calibration period, the model performances are worst as confirmed by Nash-Sutcliffe index value of 0.21 with respect to the value of 0.65 estimated for the calibration period. In addition, the simulation fails in reproducing the most extreme values: high flows in winter and spring are underestimated and summer discharges are overestimated, as results the average discharges in winter-spring are underestimated and those in summer-autumn overestimated, as shown in Fig. 12. However, a partial justification of the low performances of the simulation in the validation period may lie in the change seen in the precipitation-discharge relationships across the 1980-1986 period that the model is not able to reproduce.

As attempt to improve the performances of the hydrological model for the case, we exchange the calibration and the validation period, thus the model is calibrated over the 1983-1993 period and validated over 1972-1982. The aim of this attempt is to verify if the calibration based on the most recent available period can provide acceptable results also on 1972-1982 pe-

Run	Horizontal Permeability at Saturation [$10^{-5}m/s$]	Vertical Permeability at Saturation [$10^{-8}m/s$]	Vertical Non-Linear Reservoir Exponent [-]
V1	2	4	12

Table 3

Soil parameters for simulation V1

Run	RMSE	RMSE-MAE	R2	NS
D1 1983-1993	2.9	1.8	0.74	0.25
V1 1983-1993	2.6	1.5	0.78	0.36

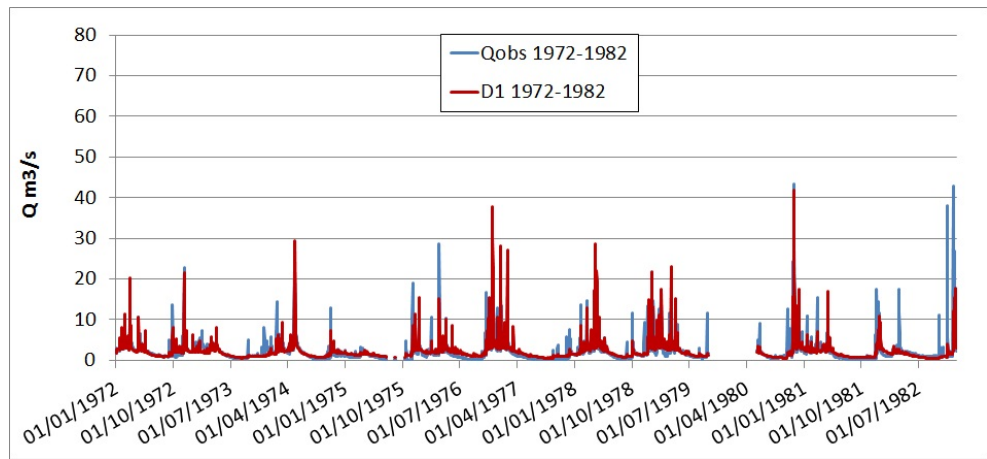
Table 4

Statistical indices for calibration run D1 and V1 from 1983 to 1993

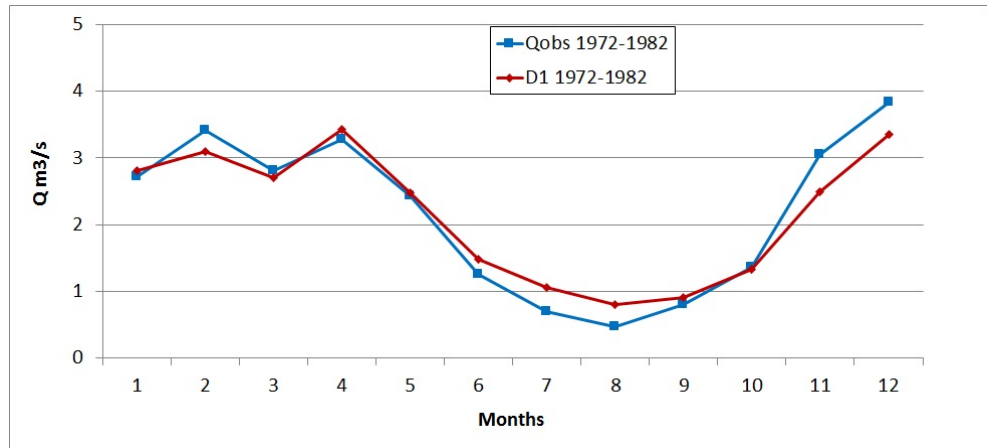
riod. The identified parameter set is reported in Tab. 3 while the comparison between observed and simulated daily and monthly discharges in the calibration (a) and validation (b) period is given in Figs 13 and 14, respectively. The performances of V1 simulation are evaluated in terms of RMSE, RMSE-MAE, R2, NS indices, Tab. 4). Unfortunately the results show that the V1 parameters set is "good" in the calibration period and only "sufficient" in the validation one.

5. CLIMATE SIMULATIONS

Climate projections are the results of numerical simulations performed by climate models under different scenarios. Among the IPCC scenarios we focus on the representative concentrations pathways RCP4.5 and RCP8.5 [17]. The first is a stabilization scenario leading the radiative forcing at about $4.5W/m^2$ in 2100, while the latter is a more extreme scenario, leading radiative forcing up to $8.5W/m^2$ in 2100 compared to pre-industrial era. Such scenarios are used to drive the global climate model CMCC-CM [27, 11] that is dynamically downscaled by the regional climate model COSMO-CLM [25] that provide climate variables at an horizontal resolution of 0.0715° (about 8 km), comparable with



(a)



(b)

Figure 11:
Comparison between observed and D1 simulated daily discharge time series (a) and monthly averages (b) in the calibration period

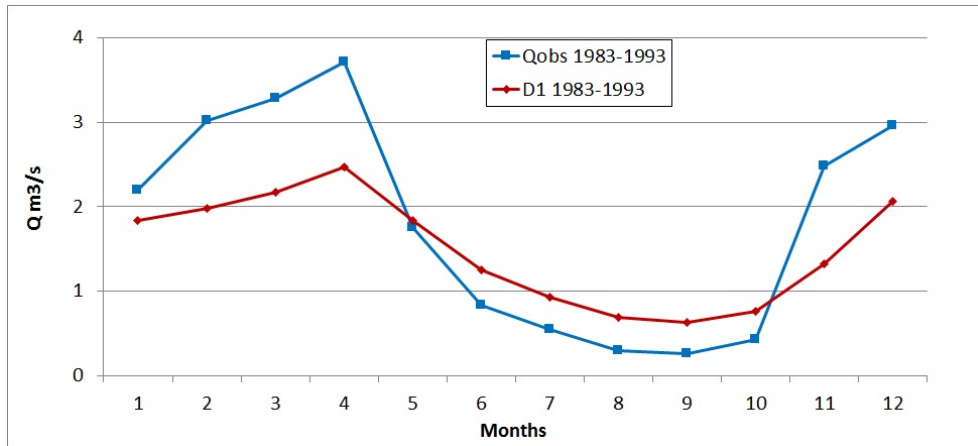


Figure 12:

Comparison between observed and D1 simulated monthly average discharge in the validation period

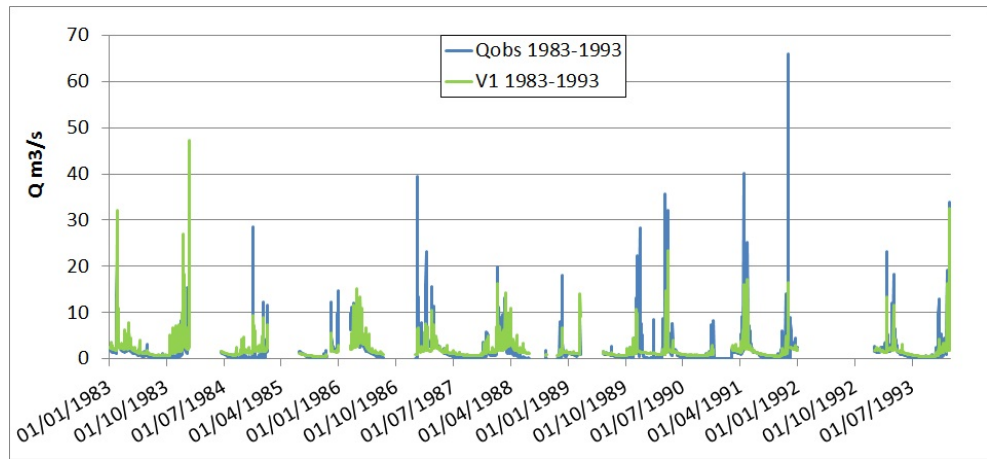
the one of the geo-hydrological hazard models.

Within GEMINA project the focus has been mostly on precipitation and temperature values [32, 33, 41, 24, 35, 37], because of their key role in the hydrological cycle [14] that regulates the occurrence of geo-hydrological hazards. Furthermore, adequate (for length, resolution and quality) observed datasets required for implementation of statistical methods are often not available for variables other than precipitation and temperature.

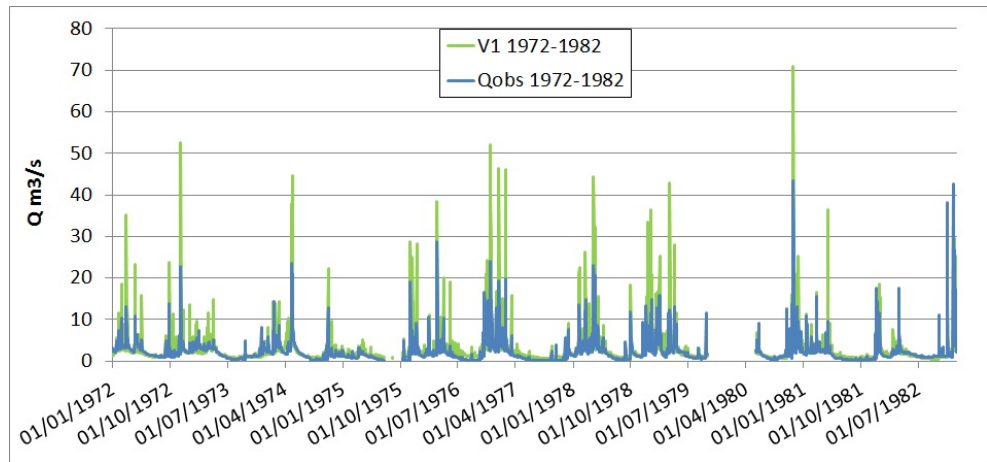
5.1 BIAS CORRECTION OF THE CLIMATE DATA

Figures 15 and 16 report the behaviour of climate simulations over the period 1972-1993 in terms of average monthly precipitation and temperature time series at Montella station, respectively. Since climate variables are essentially investigated at point scale (represented by Montella station) while the effective resolution of the RCM can be assumed about equal to 3-7 the nominal resolution [28, 1, 15] we used as effective resolution $3\Delta x$, thus simulated climate variables are the average values

on a 3×3 grid centred on Montella site, additionally daily precipitation values lower than 0.01 mm/day have been treated as null precipitation. As shown, CMCC-CM/COSMO-CLM variables are affected by a systematic bias caused by, e.g., uncertainty in the GCM/RCM parametrizations or assumptions, which has to be removed before performing quantitative evaluations on hydrological or other impacts [29]. A description of the different bias correction techniques implemented in Clime software and based on the *qmap* R-package [12] is reported in [38, 20] while other bias correction techniques like linear scaling and analogs are described in [41, 34, 32, 33]. As explained in [20] and shown in Fig.15 the comparison between the observed, CMCC-CM/COSMO-CLM, with and without, precipitation shows that CMCC-CM/COSMO-CLM reproduces correctly the seasonality but values are underestimated, and considering the bias correction methods parametric quantile-quantile and non parametric techniques outperform the distribution derived transformations, but non parametric techniques show a overestimation of the occurrence of precipitation lower than 5 mm/day,

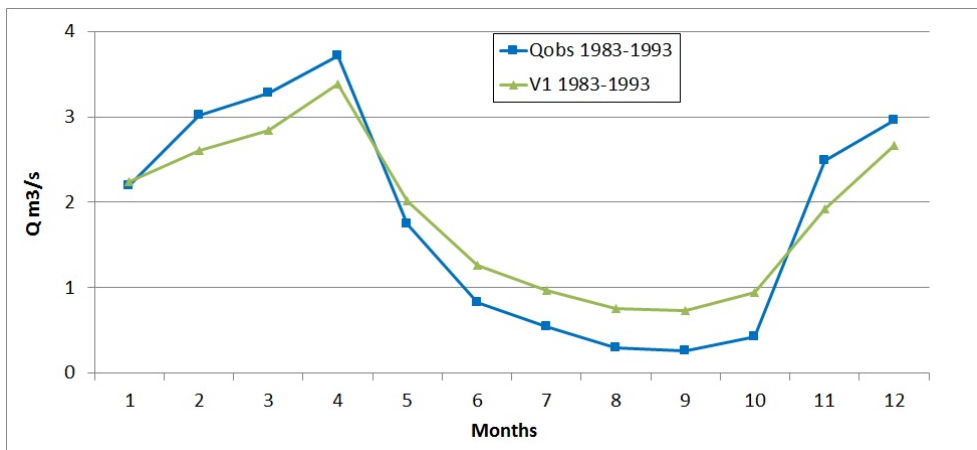


(a)

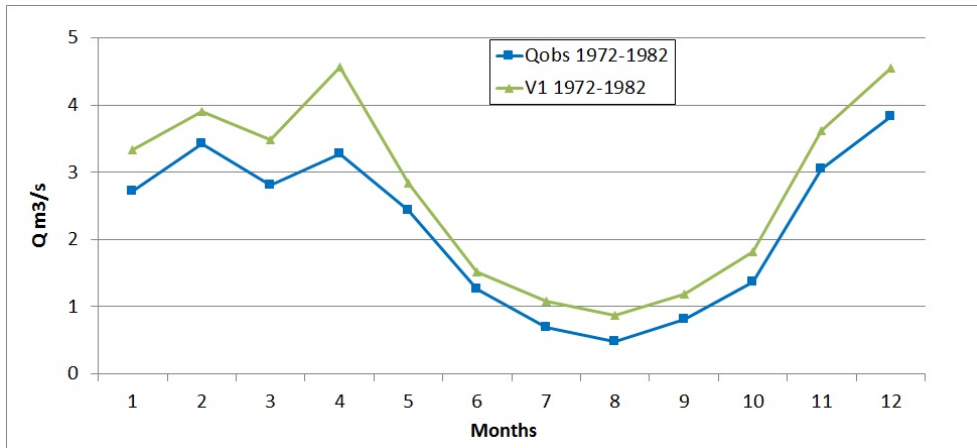


(b)

Figure 13: Comparison between observed and simulated daily discharges in the calibration (a) and validation (b) periods for V1 simulation



(a)



(b)

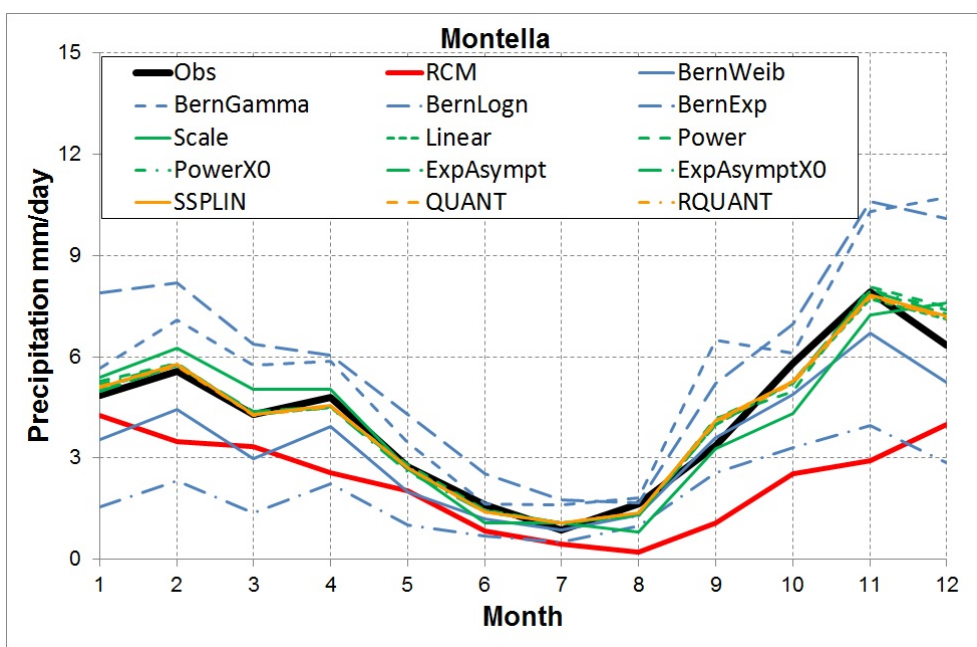
Figure 14:
As Fig. 13 but for monthly average discharges

Fig. 15(a,b). For temperature, Fig. 16, CMCC-CM/COSMO-CLM is characterised by a general underestimation of average monthly values that is reflected in the cumulative distribution function (CDF); non parametric techniques seems to reproduce better the observed temperature than parametric quantile-quantile approaches with the exception of Linear, ExpAsympt and ExpAsympt.X0 methods that have performances comparable to non parametric techniques. In terms of CDFs the highest similarity with the one of observed temperature is found for: Linear, ExpAsympt.X0, QUANT, RQUANT, SSPLIN methods.

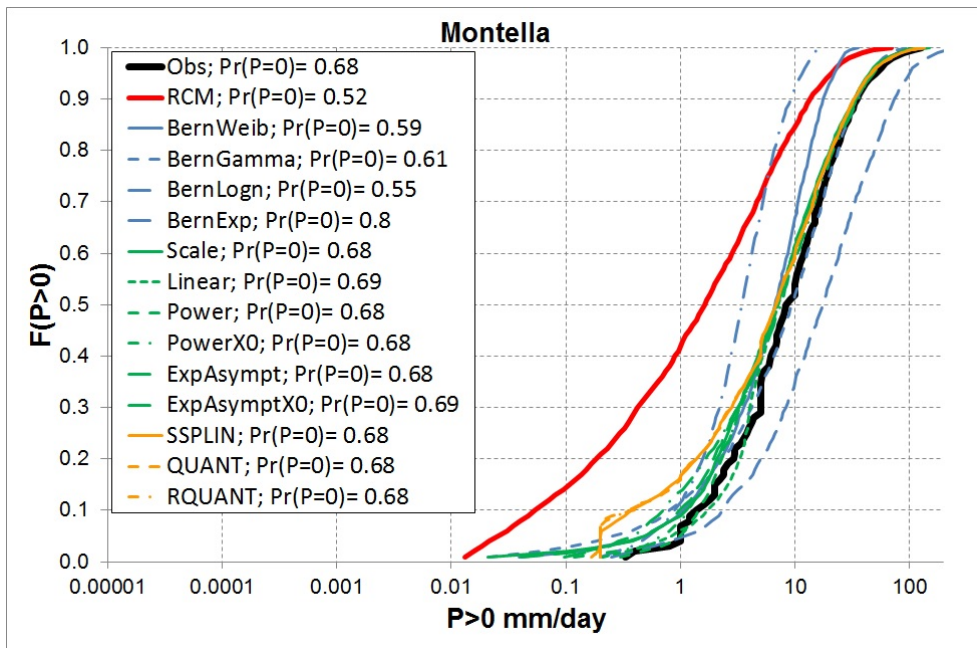
5.2 CLIMATE PROJECTIONS

Once assessed the performances of the GCM/RCM couple in reproducing the observed climate it is possible to investigate the effects of IPCC scenarios on climate evolution. In particular, we will focus on three different periods: short (2021-2050), medium (2041-2070) and long (2071-2100) term under RCP4.5 and RCP8.5 [17]. For these analysis, the 30 years long period, 1972-2001, is considered as reference to estimate the monthly anomalies in precipitation (Fig.s 17-19) and temperature (Fig.s 20-22) at 2021-2050 (Fig.s 17 and 20), 2041-2070 (Fig.s 18 and 21) and 2071-2100 (Fig.s 19 and 22) under both RCP4.5 and RCP8.5. Figures 17-22 report the estimated anomalies for precipitation and temperature, respectively. First of all, the shape of precipitation anomaly is quite consistent comparing raw and bias corrected data: a reduction of precipitation is projected in all month with the exception of August and only the SSPLIN method indicates a positive anomaly in March. For temperature, it is worth to note that bias corrected time series are characterised by positive anomalies higher than CMCC-CM/COSMO-CLM data; as for precipitation, there is a general agreement in the

shape of the anomalies but, SSPLIN simulates a really high anomaly ($>10^{\circ}\text{C}$) in August. This behaviour is due to (1) the fact that bias correction methods are not physically based and (2) the occurrence in 2071-2100 of temperature values outside the calibration range of SSPLIN method, thus a linear relationship is used to extrapolate the bias corrected value. Since the anomaly shown by SSPLIN temperature appears to be too extreme, SSPLINE bias corrected data will not be used to drive the hydrological model. Note that considering the control period only, SSPLIN method is among those performing better.



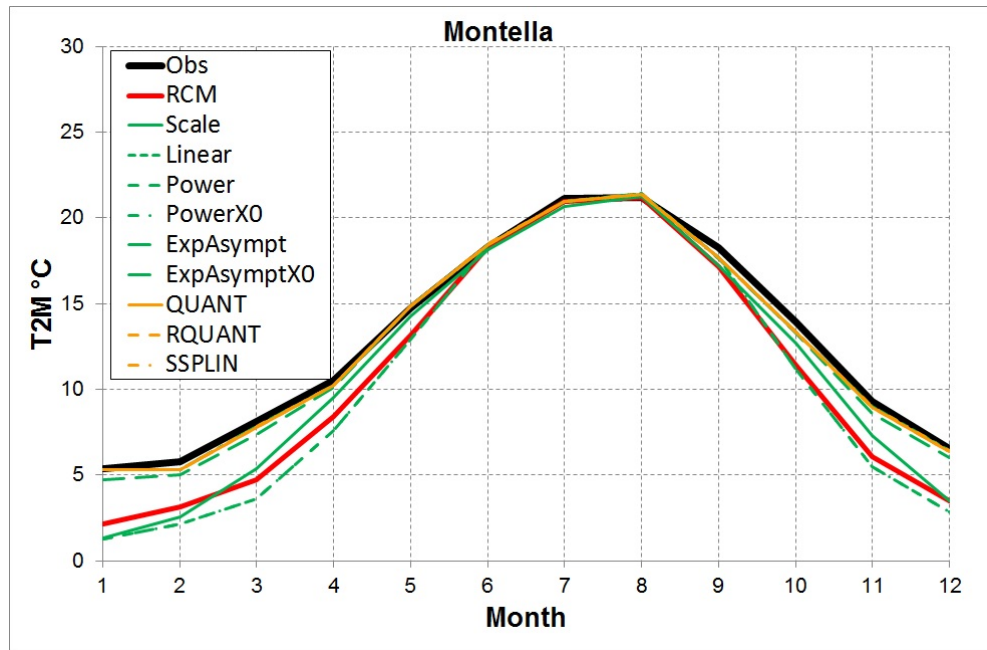
(a)



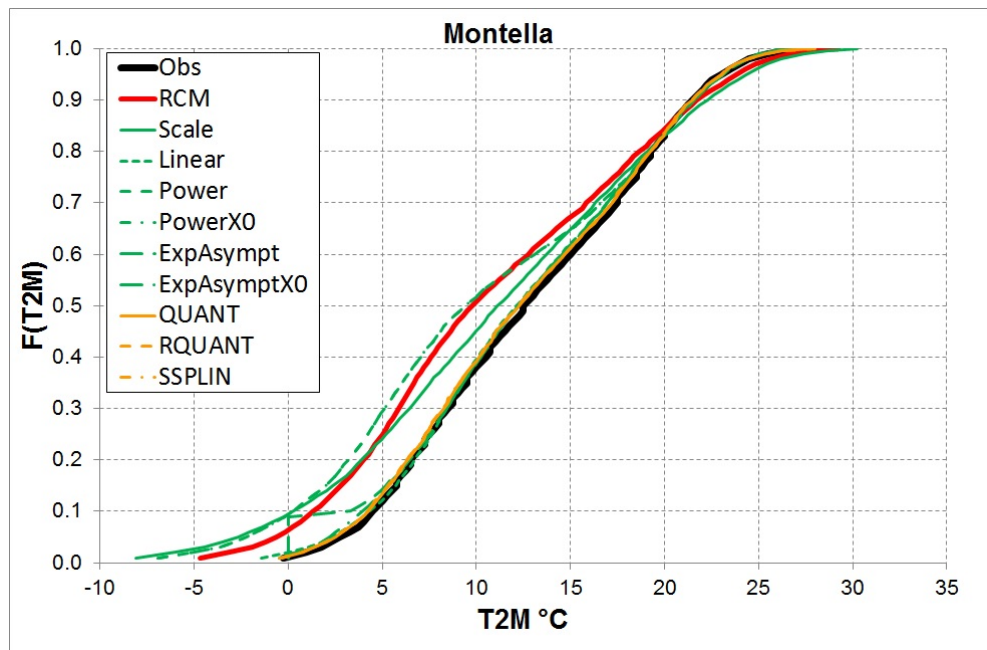
(b)

Figure 15:

Comparison among observed, GCM/RCM simulated and bias corrected precipitation data. Panels refer to (a) monthly averages and (b) empirical CDFs. Blue: Distribution derived transformation; Green: Parametric quantile-quantile; Orange: Non parametric methods

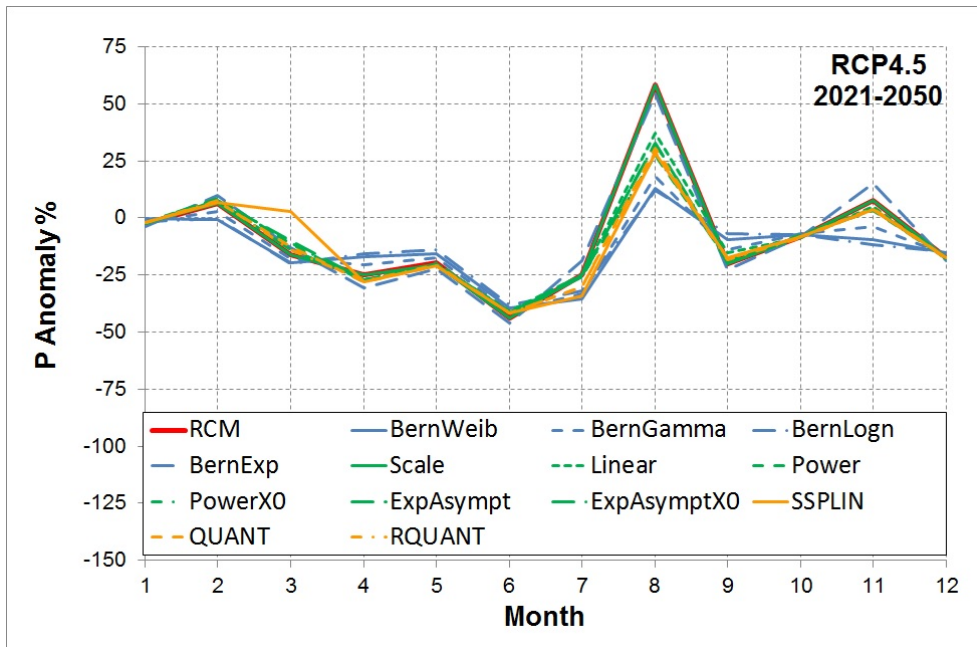


(a)

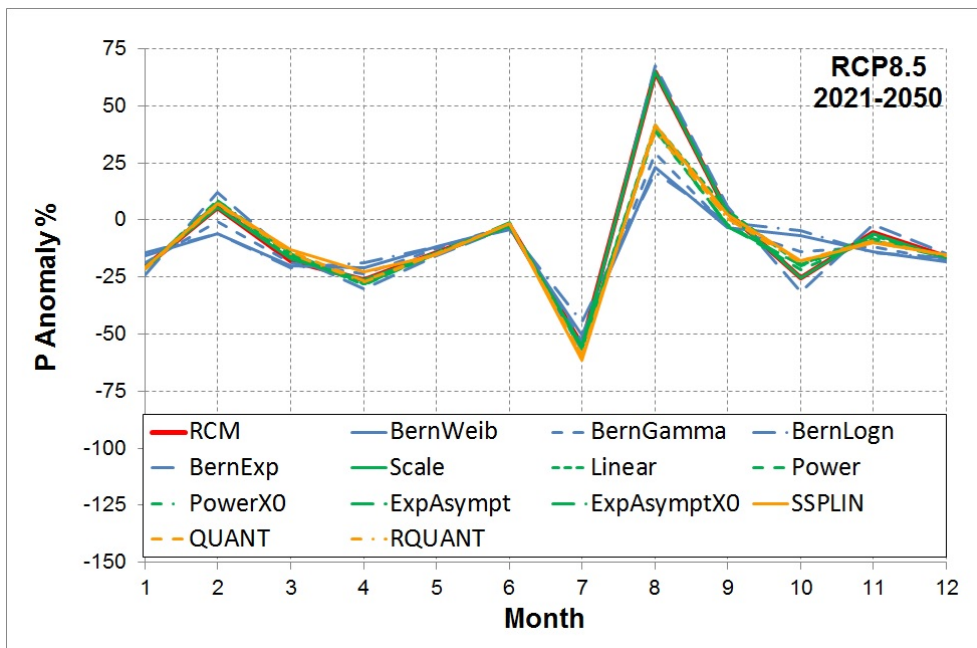


(b)

Figure 16:
As Fig.15 but for temperature

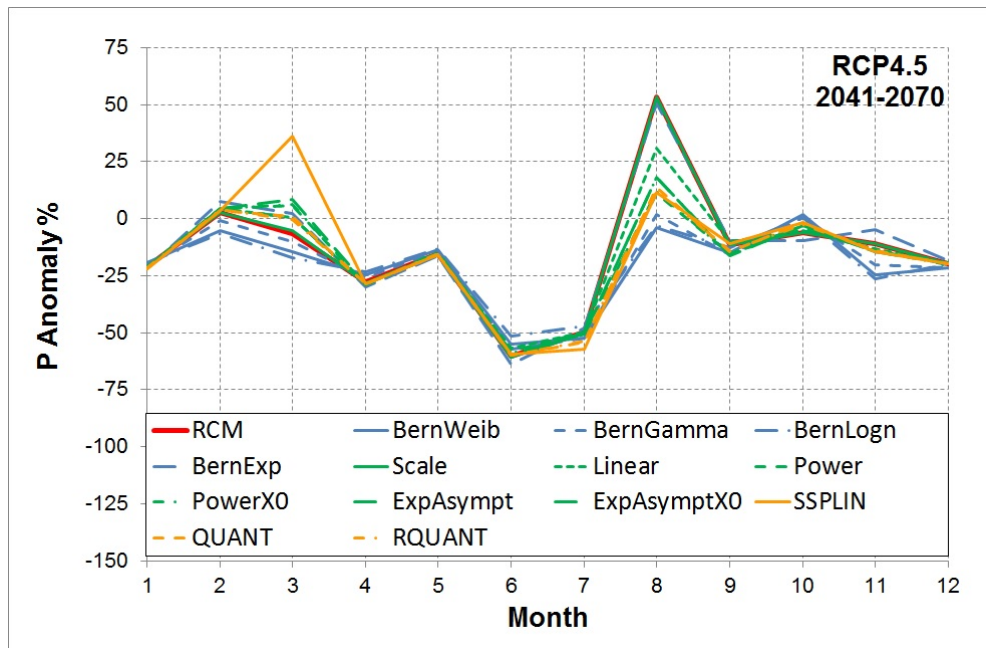


(a)

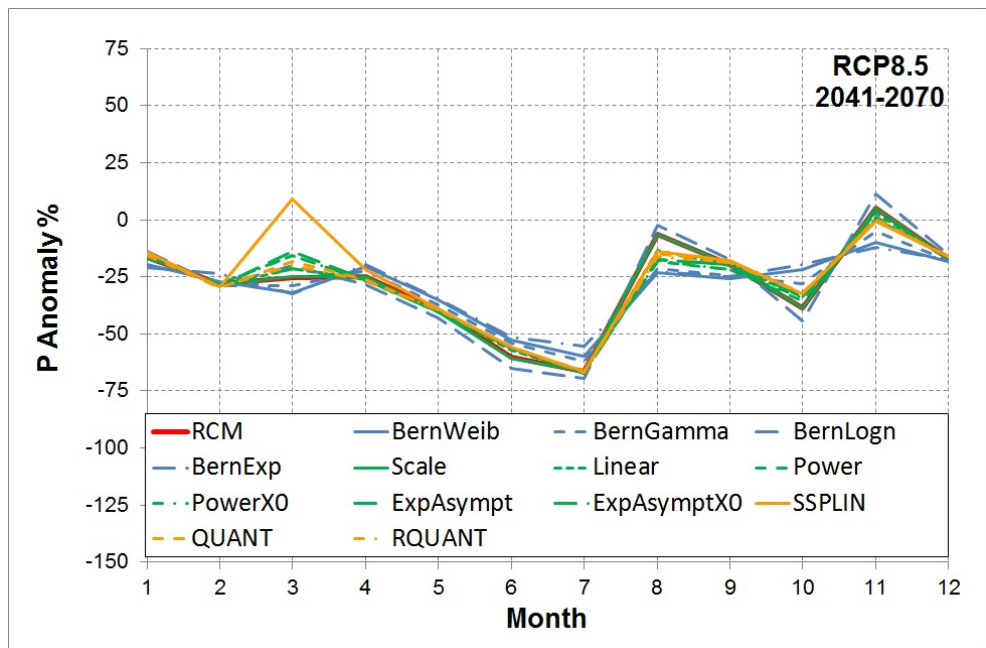


(b)

Figure 17: Comparison among monthly average precipitation anomalies for period 2021-2050 (in %) obtained for CMCC-CM/COSMO-CLM simulated and bias corrected data. (a) RCP4.5 and (b) RCP8.5 scenarios. Red: CMCC-CM/COSMO-CLM; Blue: Distribution derived transformation; Green: Parametric quantile-quantile; Orange: Non parametric methods

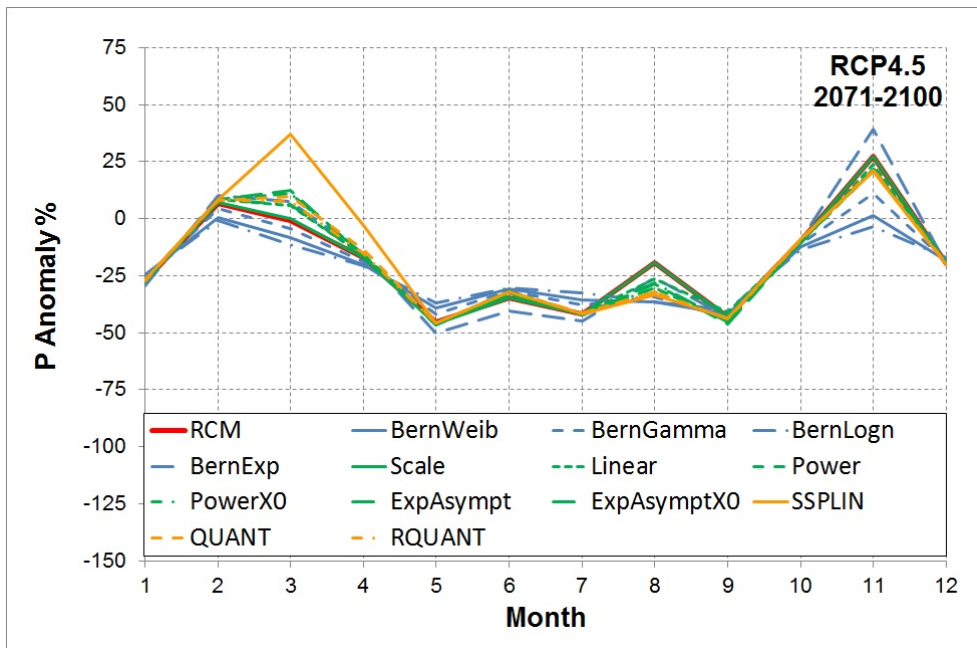


(a)

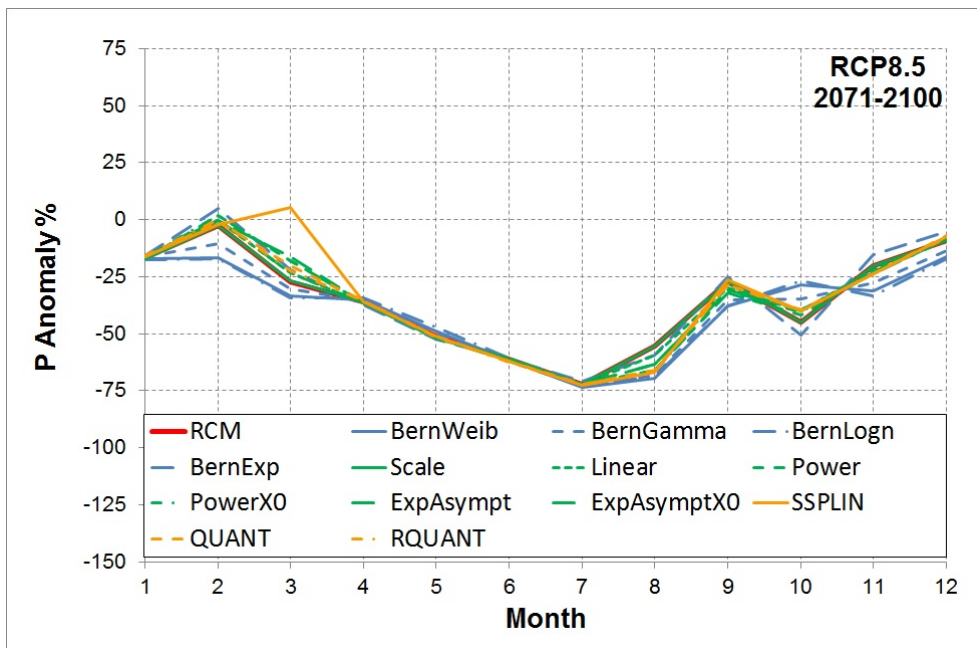


(b)

Figure 18:
As Fig. 17 but for 2041-2070

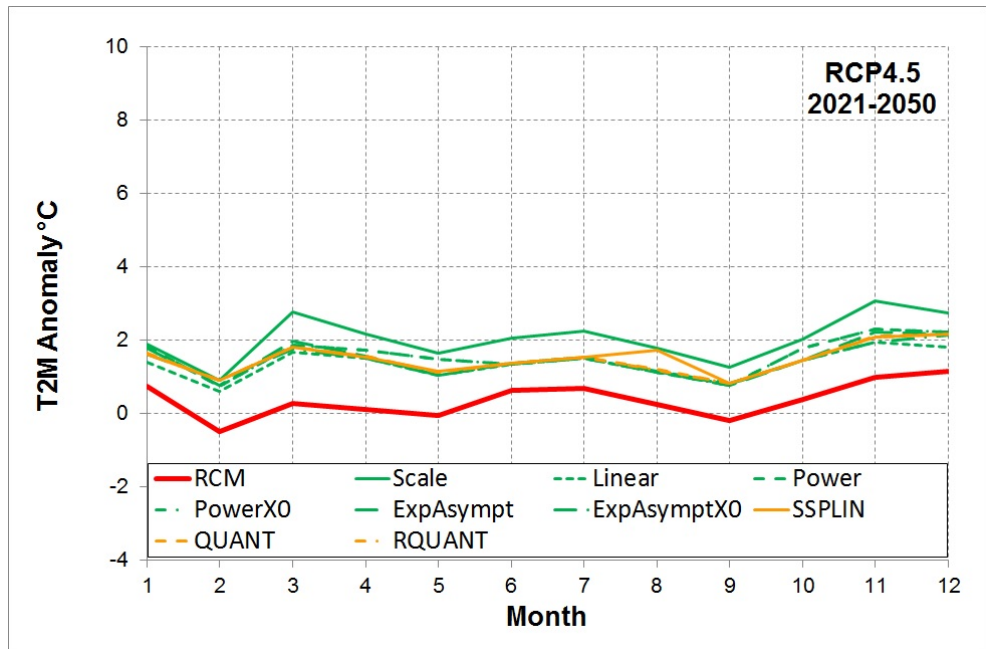


(a)

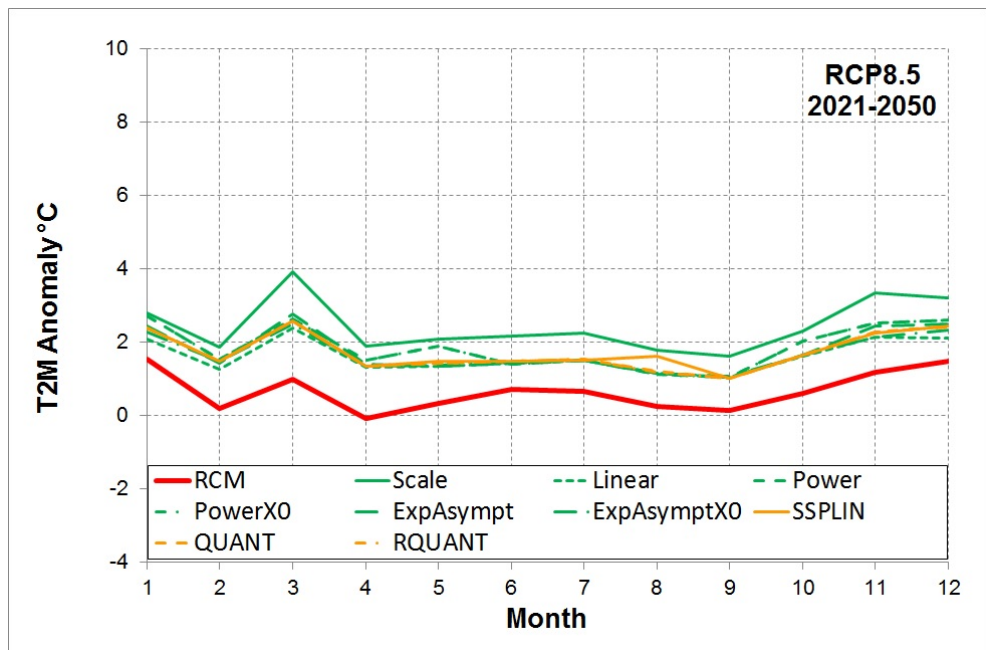


(b)

Figure 19:
As Fig. 17 but for 2071-2100

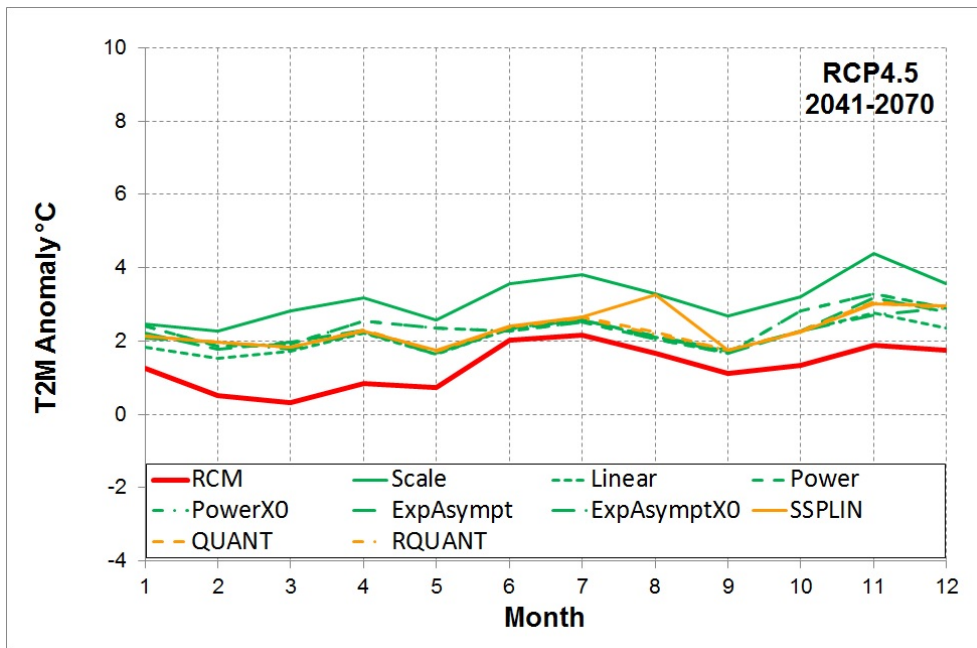


(a)

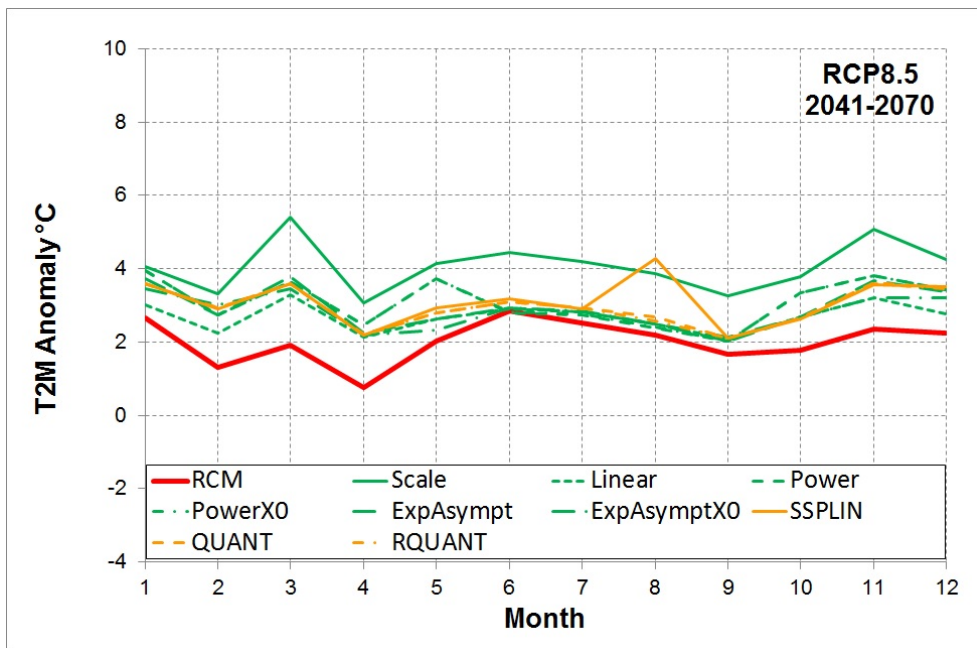


(b)

Figure 20: Comparison among monthly average temperature anomalies for period 2021-2050 (in °C) obtained for CMCC-CM/COSMO-CLM simulated and bias corrected data. (a) RCP4.5 and (b) RCP8.5 scenarios. Red: CMCC-CM/COSMO-CLM; Blue: Distribution derived transformation; Green: Parametric quantile-quantile; Orange: Non parametric methods

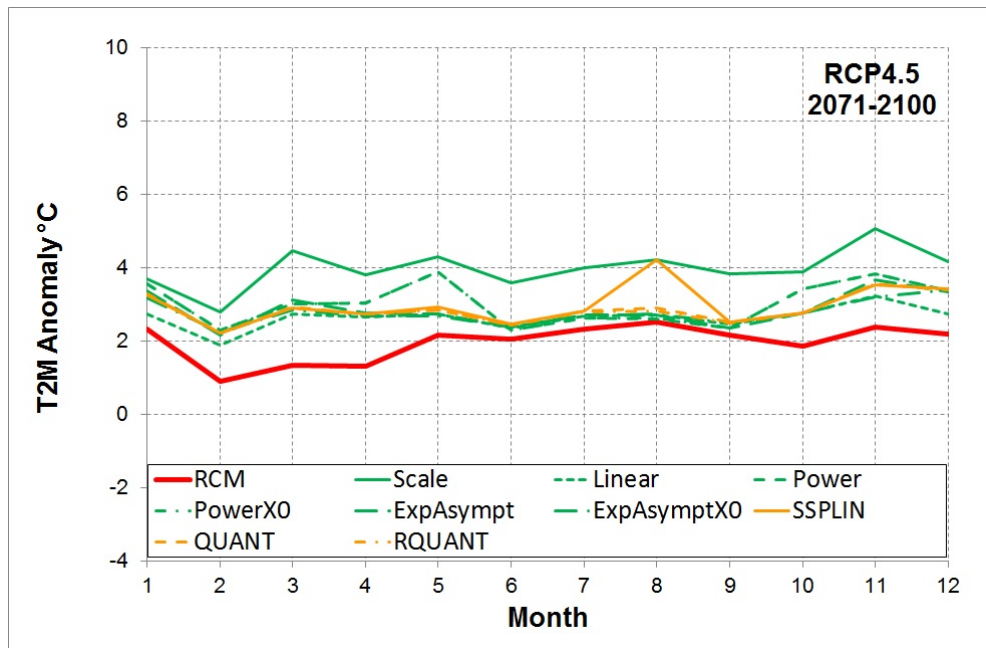


(a)

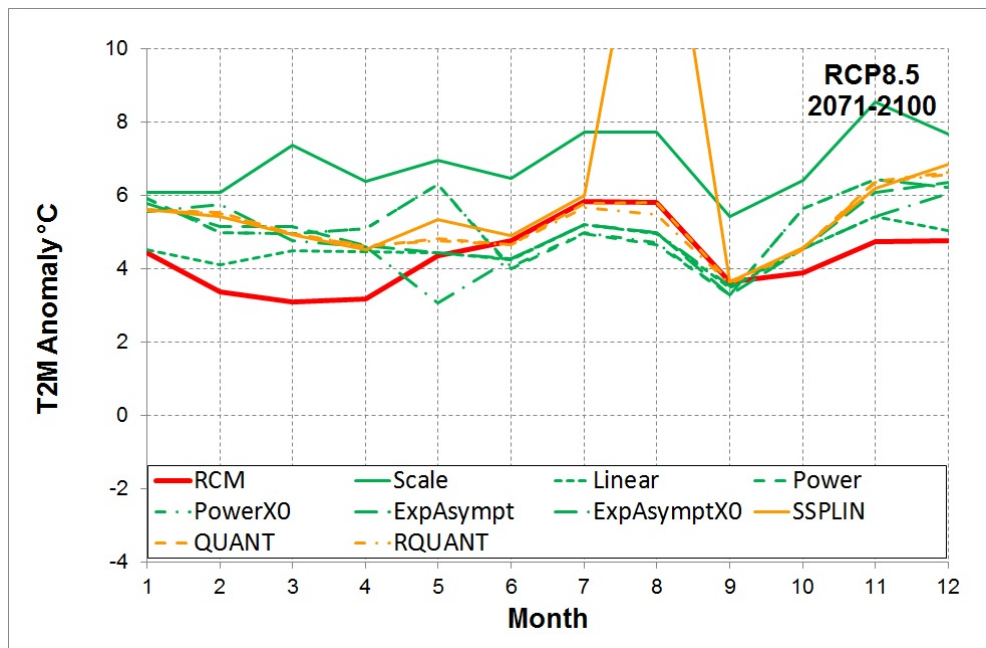


(b)

Figure 21:
As Fig. 20 but for 2041-2070



(a)



(b)

Figure 22:
As Fig. 20 but for 2071-2100



6. CLIMATE-HYDROLOGICAL SIMULATIONS

The hydrological cycle of Calore Irpino River basin closed at Montella cross section is simulated through forcing TOPKAPI with simulated (and bias corrected) precipitation and temperature time series. The hydrological model returns, among others, the estimated: discharge (m^3/s), net precipitation (mm), snow (mm), potential and actual evapotranspiration (mm), percolation (mm), surface runoff (mm), and soil saturation (%). The effects of bias correction on values of this components of the hydrological cycle on the control period have been investigated in [20]. In the next Sections we focus on the following variables: precipitation, temperature and discharge under present and future climate conditions.

6.1 PRESENT

Once that the parametrization of the hydrological and climate models is assessed, it is possible to evaluate the performances of the whole modelling chain, i.e. the simulated discharge when TOPKAPI is driven by precipitation and temperature time series obtained from CMCC-CM/COSMO-CLM simulations or by the bias corrected variables. Figure 23 reports, for the period 1972-1993, the comparison among the observed and simulated discharges averaged at monthly timescale and the cumulative distribution function (CDF) of daily data. The control period is limited to 1972-1993 for coherence with the availability of observations.

Results show that TOPKAPI tends to overestimate the lowest discharges, that may be due to an uncorrected parametrization of the soil, that in this application, has been assumed to be the same for all the basin. Among the bias correction methods, linear, expasympt and RQUANT seem to perform better than the others com-

pared to TOPKAPI simulation driven by observed precipitation and temperature time series.

6.2 FUTURE

As done for climate projections, the analysis of the effects of RCP4.5 and RCP8.5 scenarios on discharges are investigated on the following periods: short (2021-2050, Fig. 24), medium (2041-2070, Fig. 25) and long (2071-2100, Fig. 25) term with respect to the reference period 1972-2001. Figures 24-26 report the discharge anomalies obtained driving TOPKAPI with CMCC-CM/COSMO-CLM climate inputs and those bias corrected with parametric quantile-quantile (linear, power.X0 and expasympt) and non parametric (QUANT, RQUANT) methods. All the simulations show a progressive reduction of average discharges, from -30% to -60/-70%, only in March discharges are slightly higher than in the present condition, however this is coherent with the precipitation pattern identified above.

7. CLIMATE CHANGE IMPACTS ON CALORE IRPINO RIVER EXTREME DISCHARGES

In order to illustrate the impacts of climate change on Calore Irpino River water availability, we report also some results on changes in extreme discharges under RCP4.5 and RCP8.5 scenarios. Extremely high and low flows are defined to occur when $Q > Q_7$ and $Q < Q_{300}$, respectively; the Q_7 (Q_{300}) value indicates the discharge that is exceeded, on average, for 7 (300) days a year. Both thresholds are estimated from data in the control period and will be used characterised also high and low flow under future climate conditions, Tab. 5 returns for each of the climate dataset considered the estimated thresholds values.

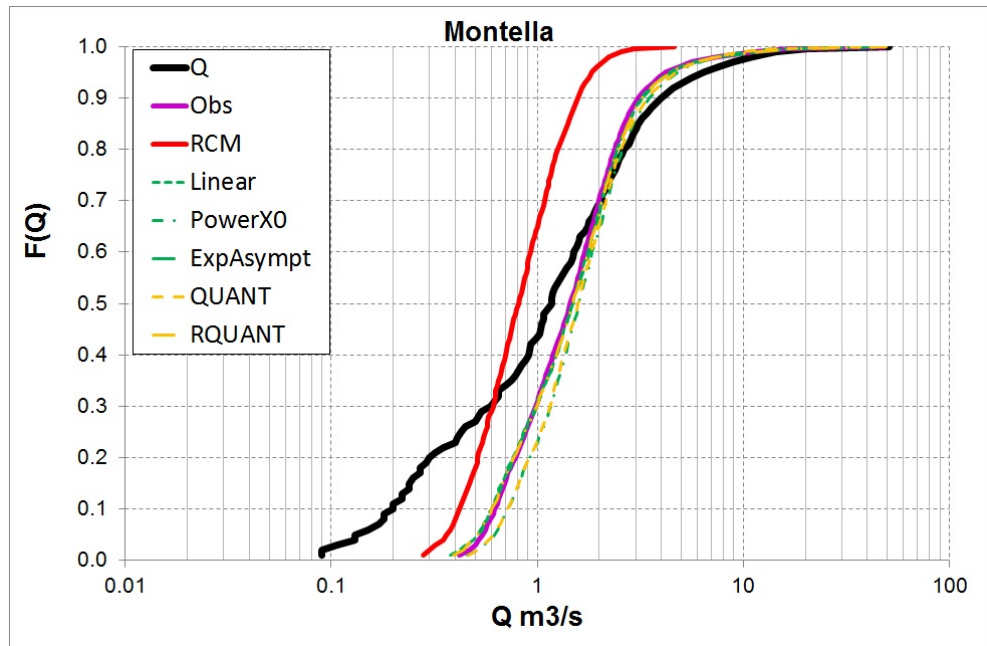
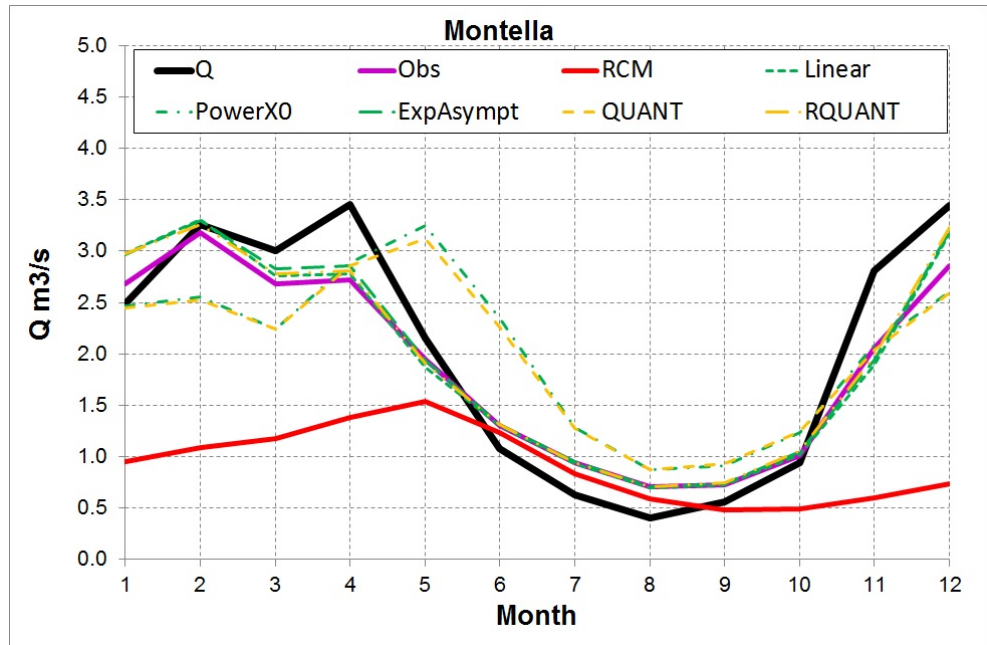
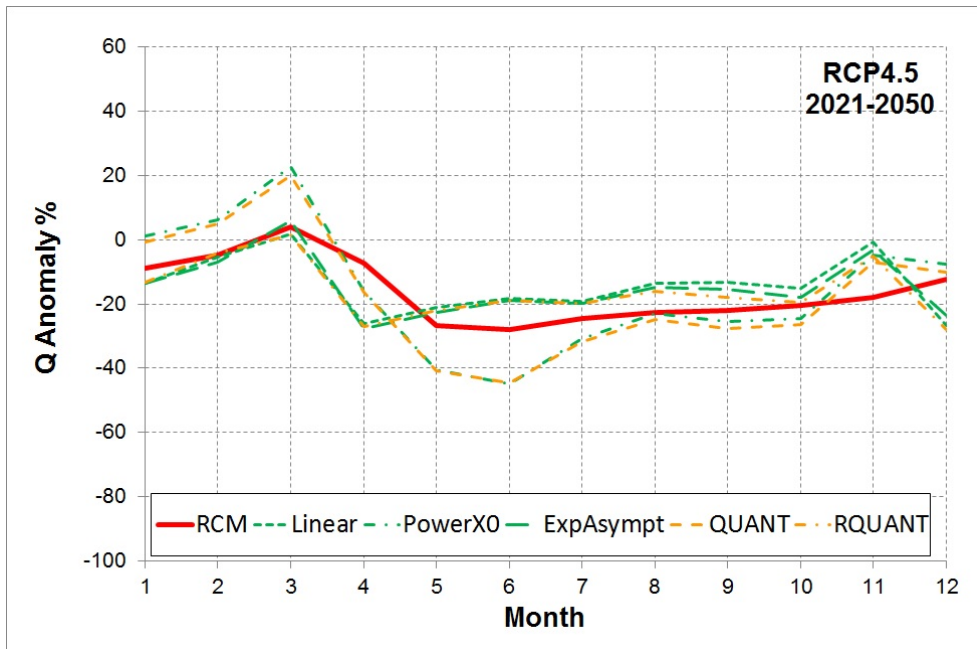
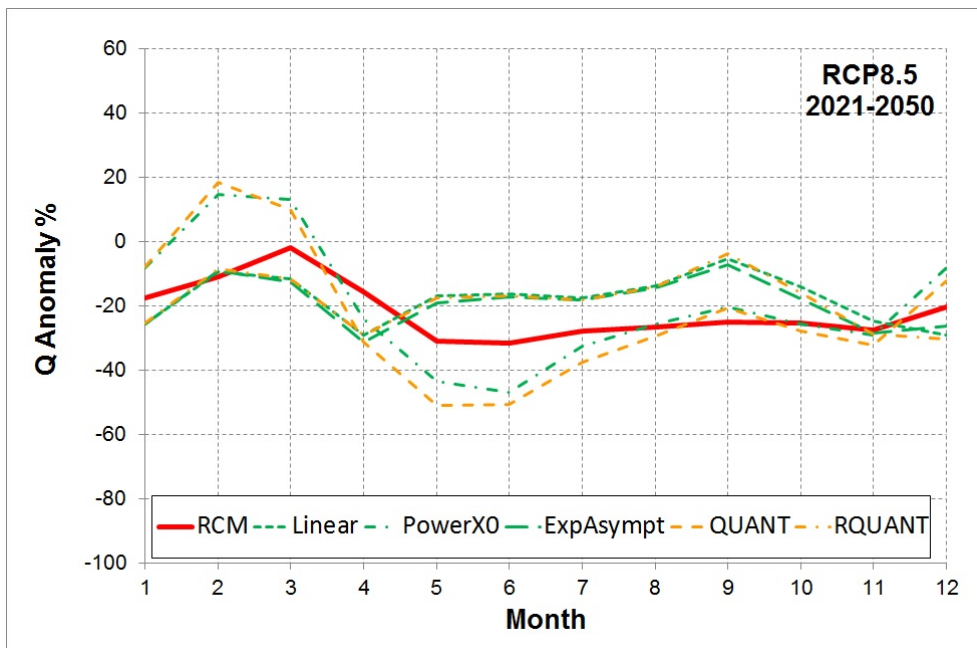


Figure 23: Comparison, over the period 1972-1993, of observed and TOPKAPI simulated discharges: (a) monthly average (b) CDF. Climate inputs to TOPKAPI are: observations (purple), raw RCM/GCM (red), bias corrected with Linear (green), Power. x_0 (green), ExpAsympt (green), QUANT (orange), RQUANT (orange) and SSPLIN (orange) approaches

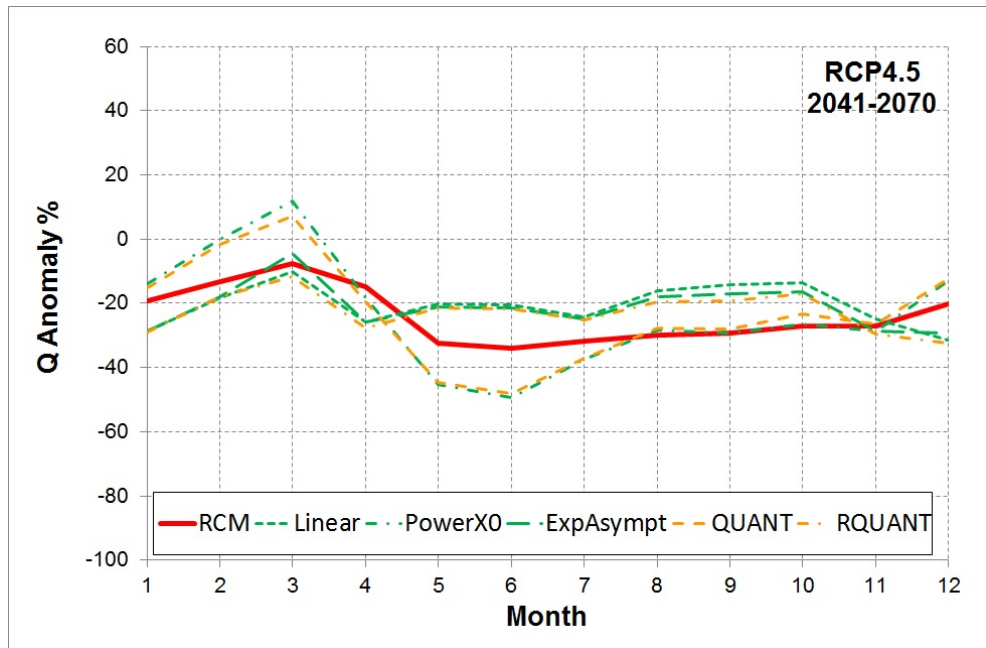


(a)

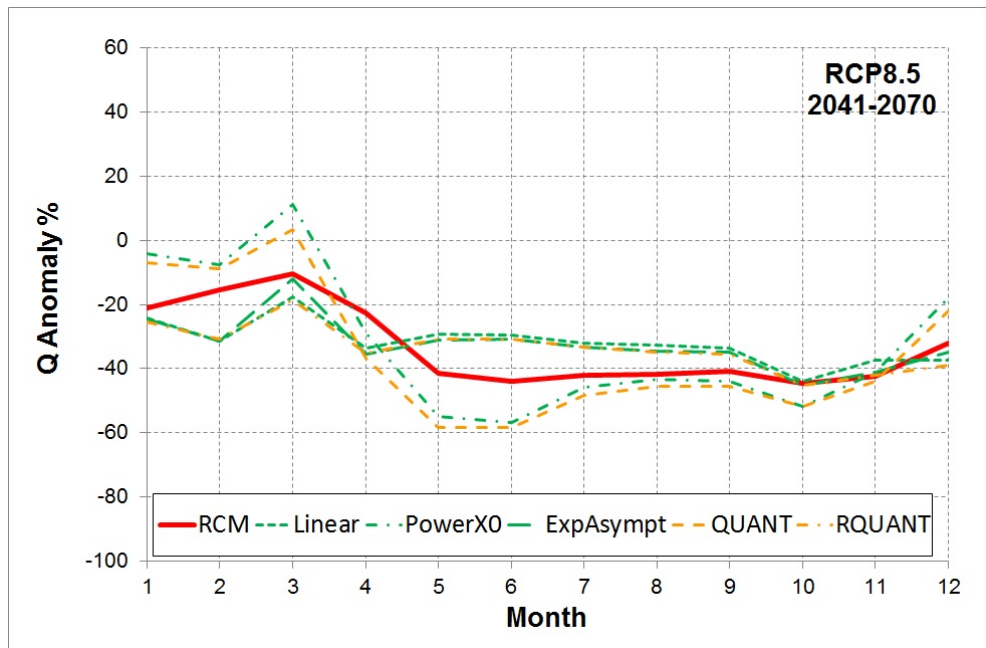


(b)

Figure 24:
Comparison among monthly average discharge anomalies (in %) at 2021-2050 obtained for CMCC-CM/COSMO-CLM simulated and bias corrected data. (a) RCP4.5 and (b) RCP8.5 scenarios. Red: CMCC-CM/COSMO-CLM; Green: Parametric quantile-quantile; Orange: Non parametric methods

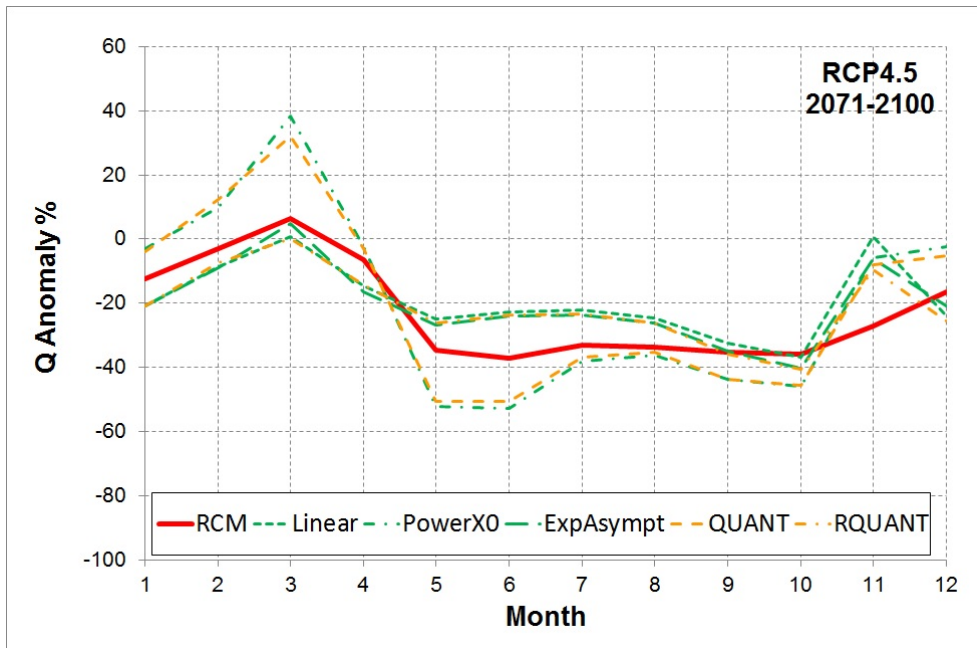


(a)

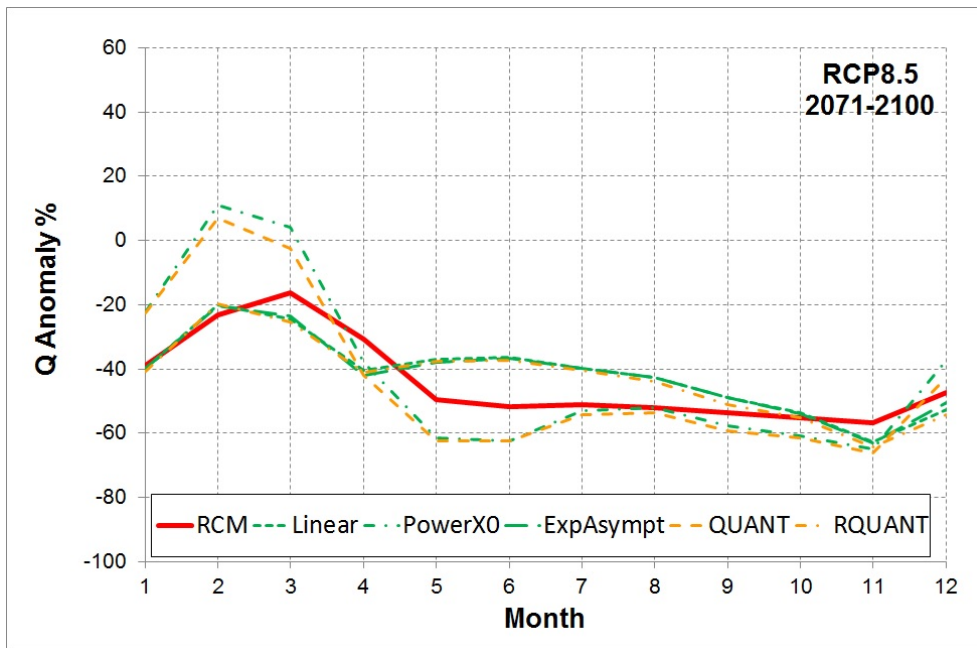


(b)

Figure 25:
As Fig. 24 but for 2041-2070



(a)



(b)

Figure 26:
As Fig. 24 but for 2041-2070



	Q_7 (m ³ /s)	Q_{300} (m ³ /s)
RCM	2.29	0.51
ExpAsympt	7.94	0.76
Linear	7.74	0.75
PowerX0	8.04	0.76
QUANT	7.77	0.90
RQUANT	7.81	0.76

Table 5

High and low flow thresholds estimated from the discharge time series obtained using raw and bias corrected climate inputs

The average volume associated to high flow (V_F) is estimated as

$$VF(i) = 86400 \times \sum_{j=1}^{N_i} \max(0, Q_j - Q_7) \quad (6)$$

where N_j is the number of day for the i -month of the year; additionally the average number of days DF such as $Q > Q_7$ can be estimated for each month.

Similarly, the low flows volume within the i -month is given by

$$VD(i) = 86400 \times \sum_{j=1}^{N_i} \max(0, Q_{300} - Q_j) \quad (7)$$

while DD returns the average number of days such as $Q < Q_{300}$.

In the control period, high flows occur mostly in winter and spring with the highest volumes associated to the spring period while low flows are mostly concentrated in summer and autumn with the maximum water deficit during summer.

According to the simulations performed, at 2021-2050, the number of high flow days (DF) is expected to decrease in almost all months as well as the volume (in particular in April and December), with the exception of March and November under RCP4.5 or during the period

November-April under RCP8.5 when the expected volume will increase, meaning that in these months high flow events could be more intense than in the control period. Figure 27 reports the estimated difference between monthly average V_F (a,b) and D_F (c,d) under RCP4.5 and RCP8.5. For the same period, low flows are projected to last for longer periods than in 1972-2001 and the associated water deficit to increase as shown in Fig. 28 that reports for all the simulations under analysis the differences between projected and control period low flows volume (a,b) and duration (c,d). In particular, the RCP8.5 scenario results to more severe than RCP4.5.

At 2041-2070 the high flow volume decreases under both scenarios in almost all the months with the exception of March, the most marked reductions of high flow volume occur between December and February and in April, the number of high flow days reduces of 1 day at the maximum with the exception of the simulation driven by raw CMCC-CM/COSMO-CLM climate data for which a reduction of about 3 days is evidenced in May. In terms of low flows, both the number of low flow days and the water deficit are increasing, in particular during summer, with respect to both 1972-2001 and 2021-2050 periods; this behaviour is more marked considering the simulations under scenario RCP8.5, Fig. 30.

At 2071-2100 the high flow volume behaviour is similar to 2021-2050 period, with increases in November, and between February and March under RCP4.5 or, for RCP8.5, between February and March only. The average number of high flow days is lower than in the control period from April to October for RCP4.5 and from April to January under RCP8.5, Fig. 31. The low flow situation become even more severe with respect to the control period and the other analysed with a persistence of low flows from



summer to winter, Fig. 32.

It is worth that the simulations driven by QUANT bias corrected climate show the highest and the longer low flows, this point need to be further investigated since it can be related to changes in the occurrence (and duration) of no-rain periods introduced by the bias correction technique; notwithstanding that the overall signal is coherent with the one obtained applying the bias correction techniques.

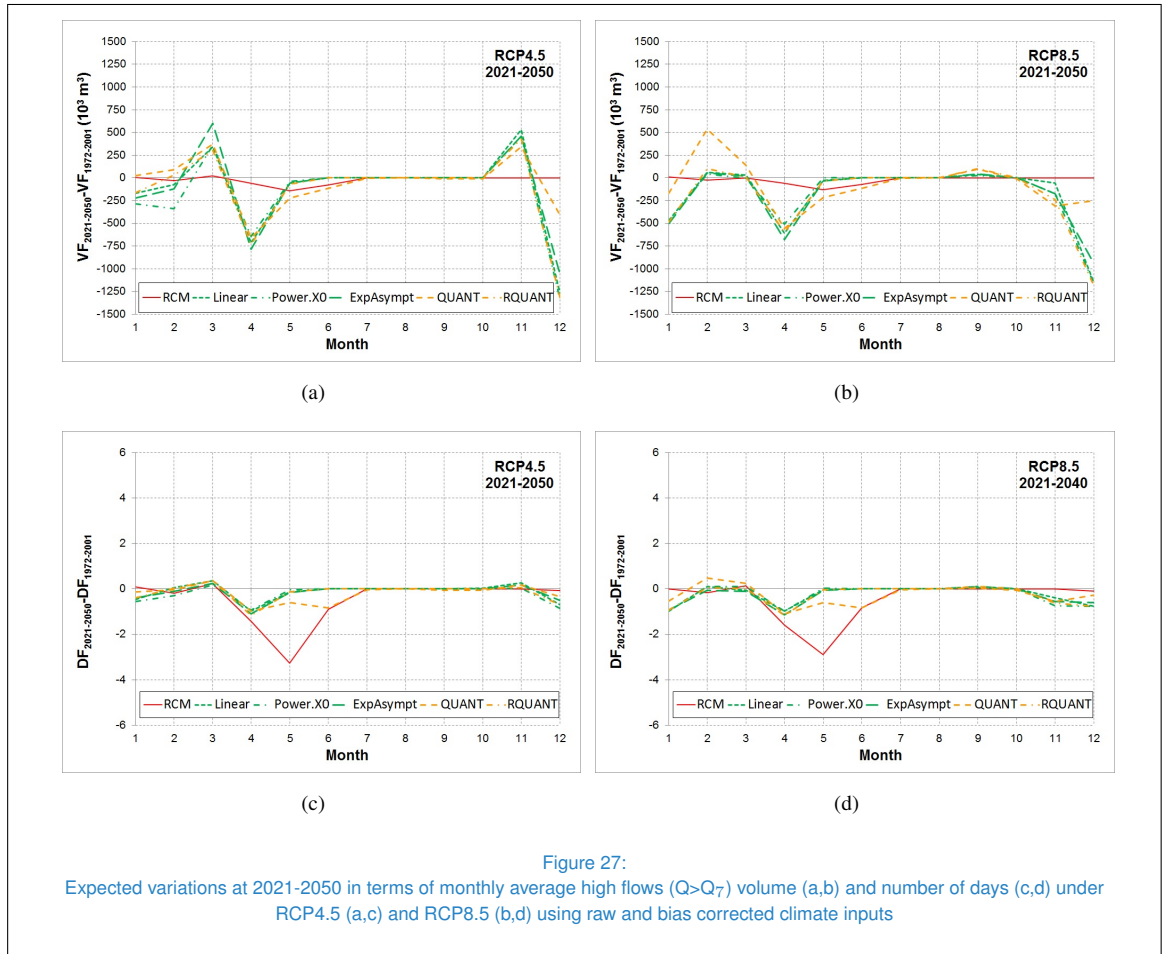


Figure 27: Expected variations at 2021-2050 in terms of monthly average high flows ($Q > Q_7$) volume (a,b) and number of days (c,d) under RCP4.5 (a,c) and RCP8.5 (b,d) using raw and bias corrected climate inputs

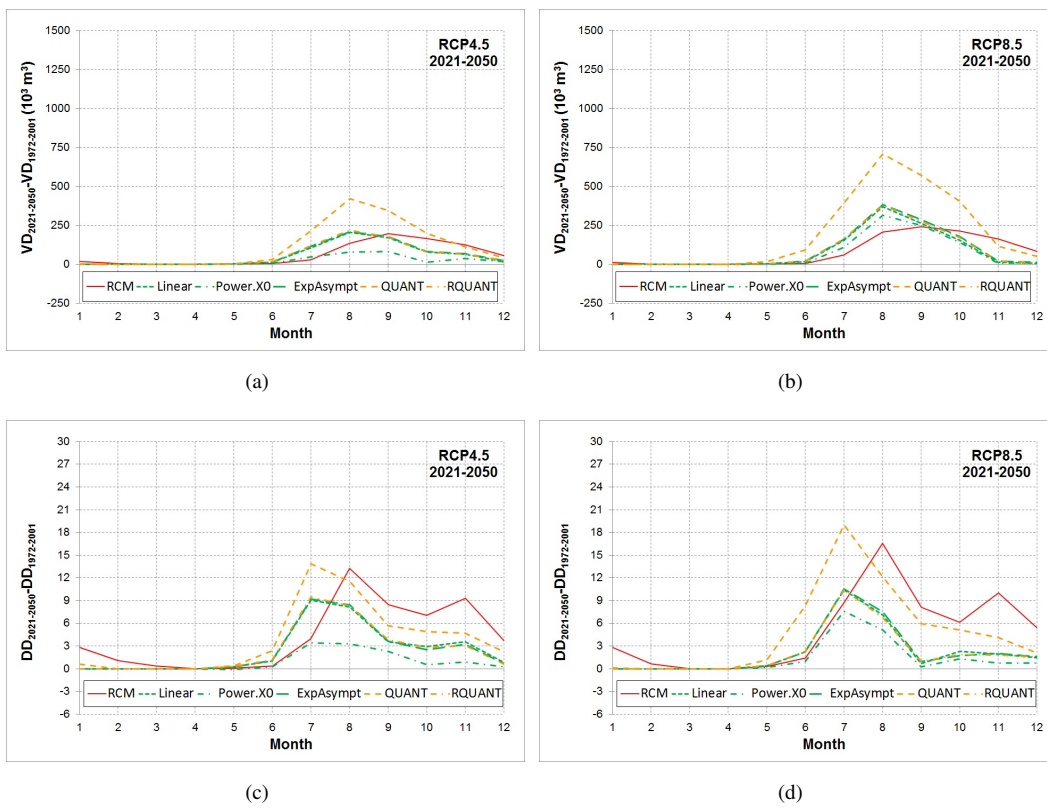


Figure 28: Expected variations at 2021-2050 in terms of monthly average low flows ($Q < Q_{300}$) volume (a,b) and number of days (c,d) under RCP4.5 (a,c) and RCP8.5 (b,d) using raw and bias corrected climate inputs

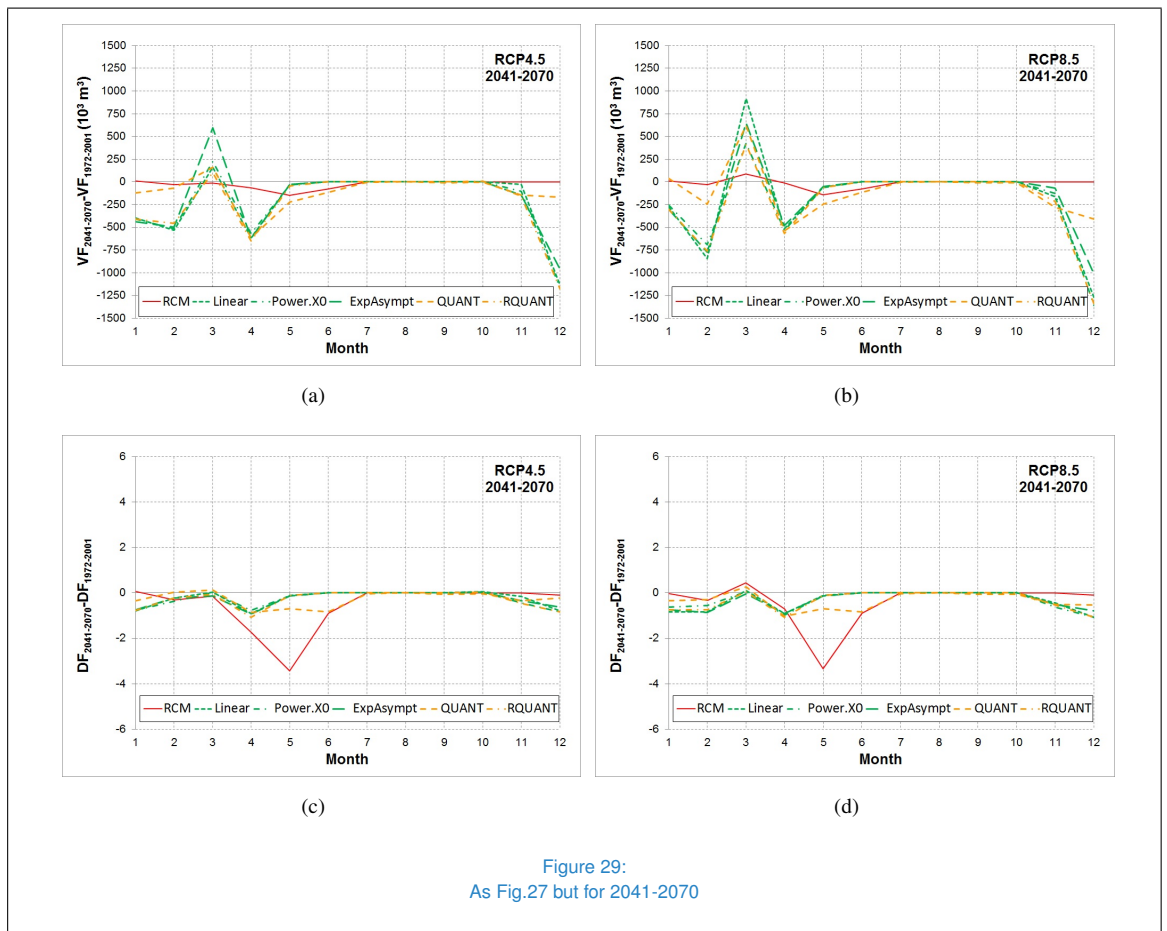
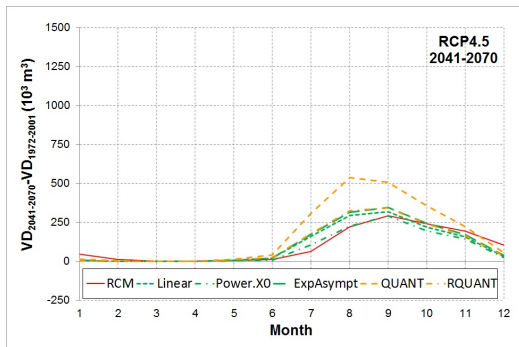
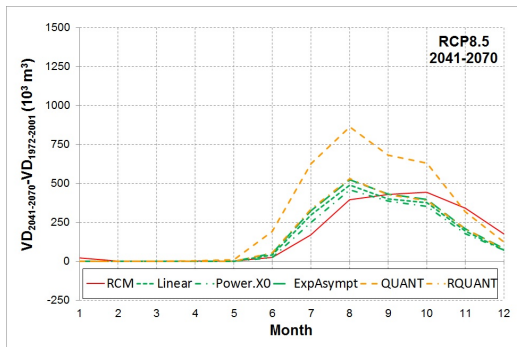


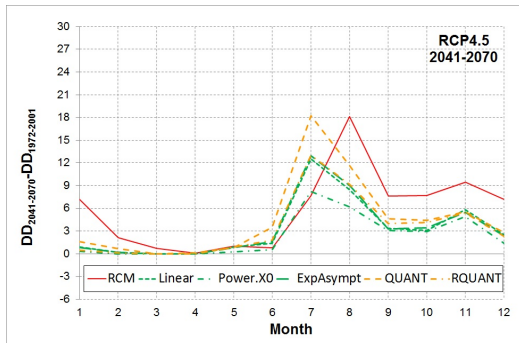
Figure 29:
As Fig.27 but for 2041-2070



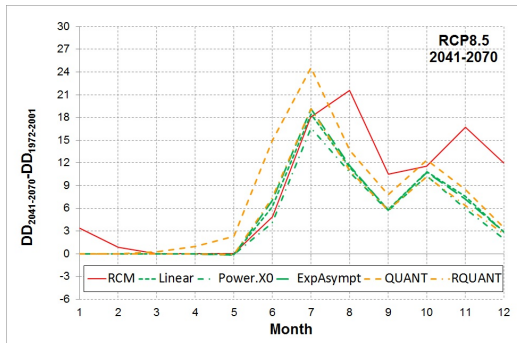
(a)



(b)



(c)



(d)

Figure 30:
As Fig.28 but for 2041-2070

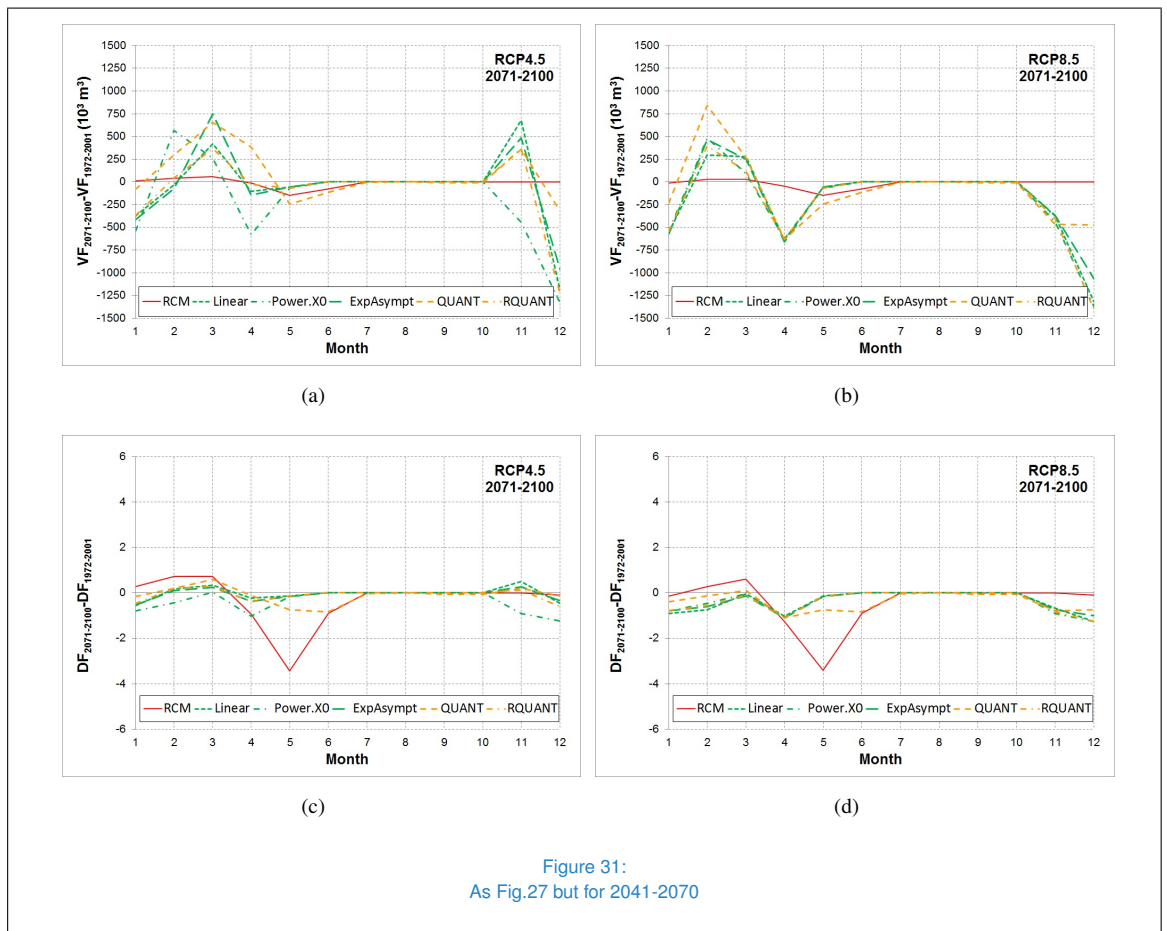
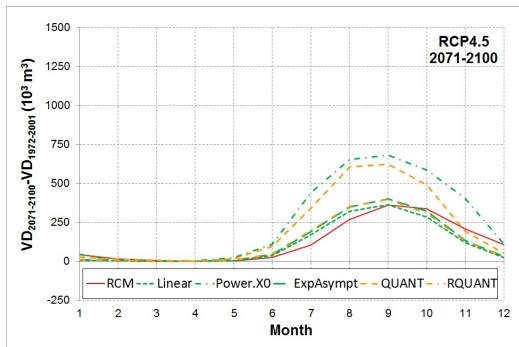
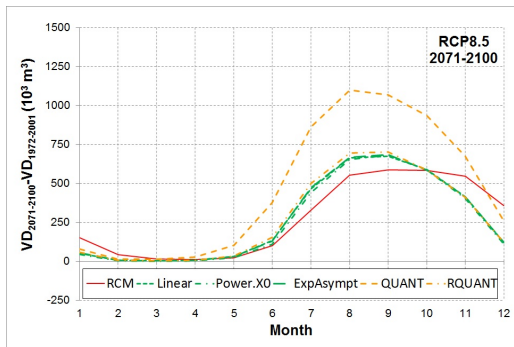


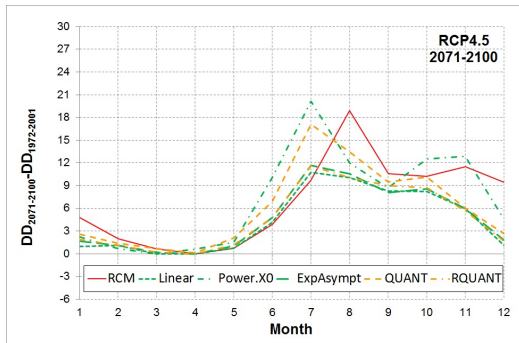
Figure 31:
As Fig.27 but for 2041-2070



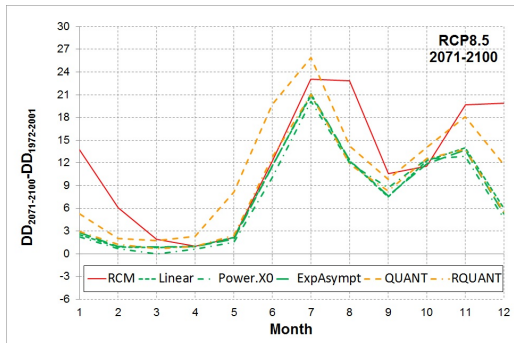
(a)



(b)



(c)



(d)

Figure 32:
As Fig.28 but for 2041-2070



8. CONCLUSIONS

The paper briefly reports and describes all the steps needed to calibrate/validate a climate-impact modelling chain and to assess climate change impacts on a river discharges.

According to the simulations performed, in the future, the area of Calore Irpino River is expected to face a reduction of water availability not only in summer, when discharges are already reduced but also in rest of the year and this it may cause problems to the agricultural production of this area. At the same time, it seems that the occurrence of high flow will reduce but the volume associated to spring events may increase, thus less but more severe events may occur in this area.

Beyond the results presented here, the Calore Irpino test case has been relevant to define

a methodology to perform climate and geo-hydrological hazards modelling and to underline some of issues related to this activity such as the “temporary” and not documented change on the hydrological response of the basin to weather forcing around the period 1982-1986 and its impacts on the calibration/validation activities. A second issue addressed is the sensitivity of the hydrological model to the climate inputs (i.e. to the bias correction technique applied), results demonstrate that, on average, non parametric techniques perform better but they should be used with attention, if data to be bias corrected fall outside the calibration range of the method. A further issue that will be taken into consideration is the development and selection of methods suitable to estimate and to reduce the overall uncertainty of the modelling chain to improve and to better communicate the achieved results.



Bibliography

- [1] L. Bierdel, P. Friederichs, and S. Bentzien. Spatial kinetic energy spectra in the convection-permitting limited-area NWP model COSMO-DE. *Meteorologische Zeitschrift*, 21(3):245–258, 2012.
- [2] S. Blenkinsop and H.J. Fowler. Changes in european drought characteristics projected by the PRUDENCE regional climate models. *International Journal of Climatology*, 27:1595 – 2610, 2007.
- [3] E. Buccignani, P. Mercogliano, M. Montesarchio, M.P. Manzi, and A.L. Zollo. Performance evaluation of COSMO-CLM over Italy and climate projections for the XXI century. In *Climate change and its implications on ecosystem and society: Proceedings of I SISC (Società Italiana di Scienze del Clima) Conference*, pages 78–89, 2013.
- [4] S. Camici, L. Brocca F. Melone, and T. Moramarco. Impact of climate change on flood frequency using different climate models and downscaling approaches. *Journal of Hydrologic Engineering*, 19(8):04014002, 2012.
- [5] L. Cattaneo, V. Rillo, M.P. Manzi, V. Villani, and P. Mercogliano. Clime: climate data processing in gis environment. *CMCC - Research Paper*, RP0257, 2015.
- [6] J.H. Christensen, B. Hewitson, A. Busuioc, A. Chen, X. Gao, I. Held, R. Jones, R.K. Kolli, W.-T. Kwon, R. Laprise, V. Magaña Rueda, L. Mearns, C.G. Menéndez, J. Räisänen, A. Rinke, A. Sarr, and P. Whetton. *Climate Change 2007: The Physical Science Basis. Contribution of Working Group I to the Fourth Assessment Report of the Intergovernmental Panel on Climate Change*, chapter Regional Climate Projections. Cambridge University Press, Cambridge, United Kingdom and New York, NY, USA, 2007.
- [7] L. Comegna, L. Picarelli, E. Buccignani, and P. Mercogliano. Potential effects of incoming climate changes on the behaviour of slow active landslides in clay. *Landslides*, 10(4):373–3091, 2013.
- [8] E. Coppola, M. Verdecchia, F. Giorgi, V. Colaiuda, B. Tomassetti, and A. Lombardi. Changing hydrological conditions in the Po basin under global warming. *Science of Total Environment*, 493:1183–1196, 2014.
- [9] E. Damiano and P. Mercogliano. *Global Environmental Change*, volume 4 of *Landslide Science and Practice*, chapter Potential effects of climate change on slope stability in unsaturated pyroclastic soils, page 499. Springer Verlag, 2013.
- [10] J. Doorembos, W.O. Pruitt, A. Aboukhaled, J. Damagnez, N.G. Dastane, C. van den Berg, P.E. Rijkema, O.M. Ashford, and M. Frere. Guidelines for predicting crop water requirements. *FAO Irrigation and Drainage Paper*, 24, 1984.
- [11] S. Gualdi, S. Somot, L. Li, V. Artale, M. Adani, A. Bellucci, A. Braun, S. Calmanti, A. Carillo, A. Dell’Aquila, M. Déqué, C. Dubois, A. Elizalde, A. Harzallah, D. Jacob, B. L’Hévéder, W. May, P. Oddo, P. Ruti, A. Sanna, G. Sannino, E. Scoccimarro, F. Sevault, and A. Navarra. The CIRCE simulations: Regional climate change projections with realistic representation of the Mediterranean Sea. *Bulletin of the American Meteorological Society*, 94:65–81, 2013.
- [12] L. Gudmundsson. *qmap: Statistical transformations for post-processing climate model output*, 2014. R package version 1.0-3.
- [13] L.N. Gunawardhana and S. Kazama. A water availability and low-flow analysis of the Tagliamento river discharge in Italy under changing climate conditions. *Hydrology*



- and *Earth System Sciences*, 16:1033–1045, 2012.
- [14] S. Hagemann, C. Chen, O.J. Haerter, J. Heinke, D. Gerten, and C. Piani. Impact of a statistical bias correction on the projected hydrological changes obtained from three GCMs and two hydrology models. *Journal of Hydrometeorology*, 12:556–578, 2014.
- [15] K.L. Kapper, H. Truhetz, and A. Gobiet. Determination of the effective resolution of regional climate models by spectral decomposition. *Proceedings 11. Österr. Klimatag*, 2010.
- [16] C. Mazzetti. TOPKAPI model references. Technical report, PROGEA, Bologna, Italy, 2014.
- [17] M. Meinshausen, S.J. Smith, K. Calvin, J.S. Daniel, M.L.T. Kainuma, J-F. Lamarque, K. Matsumoto, S.A. Montzka, S.C.B. Raper, K. Riahi, A. Thomson, G.J.M. Velders, and D.P.P. van Vuuren. The RCP greenhouse gas concentrations and their extensions from 1765 to 2300. *Climatic Change*, 109:213–214, 2011.
- [18] P. Mercogliano, M. Montesarchio, G. Rianna, P. Schiano, R. Vezzoli, and A.L. Zollo. High resolution climate scenarios on mediterranean test case areas for the hydro-climate integrated system. *CMCC Research Paper*, RP0233, 2014.
- [19] P. Mercogliano, G. Rianna, and R. Vezzoli. Frequency variation of geo-hydrological hazards under climate change conditions in italy. *CMCC - Research Paper*, RP0264, 2015.
- [20] P. Mercogliano, G. Rianna, R. Vezzoli, V. Villani, and V. Coppola. Evaluation of downscaling and bias correction techniques to link climate and geo-hydrological impacts models. *CMCC - Research Paper*, RP0263, 2015.
- [21] L. Picarelli, L. Comegna, F. Guzzetti, S.L. Gariano, P. Mercogliano, G. Rianna, M. Santini, and P. Tommasi. Potential climate changes in italy and consequences on land stability Italian contribution to JTC1 - Technical Report no 3 (TR3) on Slope Safety Preparedness for Effects of Climate Change. Technical Report draft available, 2015.
- [22] G. Ravazzani, S. Barbero, A. Saladin, A. Senatore, and M. Mancini. An integrated hydrological model for assessing climate change impacts on water resources of the upper Po river basin. *Water Resour. Manag.*, 29:1193–1215, 2015.
- [23] G. Rianna, P. Tommasi, L. Comegna, and P. Mercogliano. Preliminary assessment of the effects of climate change on landslide activity of Orvieto clayey slope. In *Climate change and its implications on ecosystem and society: Proceedings of I SISC (Società Italiana di Scienze del Clima) Conference*, pages 507–522, 2013.
- [24] G. Rianna, A.L. Zollo, P. Tommasi, M. Paciucci, L. Comegna, and P. Mercogliano. Evaluation of the effects of climate changes on landslide activity of Orvieto clayey slope. *Procedia Earth and Planetary Science*, 9:54–63, 2014.
- [25] B. Rockel, A. Will, and A. Hense. The regional climate model COSMO-CLM (CCLM). *Meteorologische Zeitschrift*, 17(4):347–348, 2008.
- [26] Madsen S. Automatic calibration of a conceptual rainfall-runoff model using multiple objectives. *Journal of Climatology*, 235:276–288, 2000.
- [27] E. Scoccimarro, S. Gualdi, A. Bellucci, A. Sanna, P. Fogli, E. Manzini, M. Vichi, P. Oddo, and A. Navarra. Effects of tropical cyclones on ocean heat transport in



- a high resolution coupled General Circulation Model. *Journal of Climate*, 24:4368–4384, 2011.
- [28] W.C. Skamarock. Evaluating mesoscale NWP models using kinetic energy spectra. *Monthly Weather Review*, 132:3019–3032, 2004.
- [29] C. Teutschbein and J. Seibert. Regional climate models for hydrological impact studies at the catchment scale: A review of recent modeling strategies. *Geography Compass*, 4/7:834–860, 2010.
- [30] E. Todini. New trends in modelling soil processes from hillslope to gcm scales. In Howard R. Oliver and Sylvia A. Oliver, editors, *The Role of Water and the Hydrological Cycle in Global Change*, volume 31 of *NATO ASI Series*, pages 317–347. Springer Berlin Heidelberg, 1995.
- [31] E. Todini. The ARNO rainfall-runoff model. *J. Hydrology*, 175:339–382, 1996.
- [32] M. Turco, A.L. Zollo, G. Rianna, L. Cattaneo, R. Vezzoli, and P. Mercogliano. Post-processing methods for COSMO-CLM over Italy. *CMCC - Research Paper*, RP0171, 2013.
- [33] M. Turco, A.L. Zollo, V. Rillo, and P. Mercogliano. GCM driven COSMO-CLM post-processed precipitation over Italy: control and future scenarios. *CMCC - Research Paper*, RP0179, 2013.
- [34] M. Turco, A.L. Zollo, R. Vezzoli, C. Ronchi, and P. Mercogliano. Daily precipitation statistics over the Po basin: observation and post-processed RCM results. In *Climate change and its implications on ecosystem and society: Proceedings of I SISC (Società Italiana di Scienze del Clima) Conference*, pages 222–232, 2013.
- [35] R. Vezzoli, M. Del Longo, P. Mercogliano, M. Montesarchio, S. Pecora, F. Tonelli, and A.L. Zollo. Hydrological simulations driven by RCM climate scenarios at basin scale in the Po river, Italy. In A. Castellarin, S. Creola, E. Toth, and A. Montanari, editors, *Evolving Water Resources Systems: Understanding, Predicting and Managing Water-Society Interactions Proceedings of ICWRS2014*, volume 364 of *IAHS Red Book*, pages 128–133, 2014.
- [36] R. Vezzoli, P. Mercogliano, S. Pecora, M. Montesarchio, A.L. Zollo, M. Del Longo, and F. Tonelli. Evaluation of climate driven simulations of Po river flow from 1971 to 2000 through flow-duration curve indices: preliminary results. *CMCC - Research Paper*, RP0186, 2013.
- [37] R. Vezzoli, P. Mercogliano, S. Pecora, A.L. Zollo, and C. Cacciamani. Hydrological simulation of Po river (north Italy) discharge under climate change scenarios using the RCM COSMO-CLM. *Science of The Total Environment*, 521-522:346–358, 2015.
- [38] V. Villani, L. Cattaneo, A.L. Zollo, P. Mercogliano, and F. Ciervo. Climate data processing with GIS support: a complete guide to bias correction tools with CLIME software. *CMCC - Research Paper*, RP0262, 2015.
- [39] P.O. Yapo, V.J. Gupta, and S. Sorooshian. Automatic calibration of conceptual rainfall-runoff model: sensitivity to calibration data. *Journal of Climatology*, 181:23–48, 1996.
- [40] A.L. Zollo, P. Mercogliano, M. Turco, R. Vezzoli, G. Rianna, E. Bucchignani, M.P. Manzi, and M. Montesarchio. Architectures and tools to analyse the impacts of climate change on hydrogeological risk on Mediterranean area. *CMCC - Research Paper*, RP0129, 2012.



- [41] A.L. Zollo, G. Rianna, P. Mercogliano, P. Tommasi, and L. Comegna. Validation of a simulation chain to assess climate change impact on precipitation induced landslides. In K. Sassa, P. Canuti, and Y. Yin, editors, *Landslide Science for a Safer Geoenvironment*, volume 1 of *Proceedings of World Landslide Forum 3*, pages 287–292, Beijing, 2014.
- [42] A.L. Zollo, V. Rillo, E. Bucchignani, M. Montesarchio, and P. Mercogliano. Temperature and precipitation extreme events over Italy: assessment of high resolution simulations with COSMO-CLM and future scenarios. *International Journal of Climatology*, 2015.
-